In Vitro Activity Differences between Proteins of the ADF/Cofilin Family Define Two Distinct Subgroups†

Hui Chen,‡ Barbara W. Bernstein, Judith M. Sneider, Judith A. Boyle, Laurie S. Minamide, and James R. Bamburg*

Department of Biochemistry and Molecular Biology, Colorado State University, Fort Collins, Colorado 80523-1870

Received January 28, 2004; Revised Manuscript Received April 5, 2004

ABSTRACT: The actin depolymerizing factor (ADF)/cofilins are an essential group of proteins that are important regulators of actin filament turnover in vivo. Although protists and yeasts express only a single member of this family, metazoans express two or more members in many cell types. In cells expressing both ADF and cofilin, differences have been reported in the regulation of their expression, their pH sensitivity, and their intracellular distribution. Each member has qualitatively similar interactions with actin, but quantitative differences have been noted. Here we compared quantitative differences between chick ADF and chick cofilin using several assays that measure G-actin binding, actin filament length distribution, and assembly/disassembly dynamics. Quantitative differences were measured in the critical concentrations of the complexes required for assembly, in the effects of nucleotide and divalent metal on actin monomer binding, in pH-dependent severing, in enhancement of filament minus end off-rates, and in steady-state filament length distributions generated in similar mixtures. Some of these assays were used to compare the activities of several ADF/cofilins from across phylogeny, most of which fall into one of two groups based upon their behavior. The ADF-like group has higher affinities for Mg^{2+}−ATP−G-actin than the cofilin-like group and a greater pH-dependent depolymerizing activity.

Actin-binding proteins of the actin depolymerizing factor (ADF) (*1*)/cofilin (AC)[1] family are ubiquitous among eukaryotes (*1*). ACs play an essential role in regulating actin filament turnover needed for many actin-based processes in nonmuscle cells. ACs typically localize to regions of cells characterized by high actin dynamics, including neuronal growth cones, ruffling membranes, cleavage furrows of cells undergoing cytokinesis, and yeast cortical actin patches (*2*−*5*). AC proteins are essential to cell division (*6*, *7*). Yeast cells expressing mutant cofilin with reduced activity have defective filament turnover (*8*). *Xenopus* AC and *Arabidopsis* ADF1 increase the turnover rate of the actin comet tail of *Listeria monocytogenes* (*9*, *10*), and a member of the AC family is one of the essential proteins in an in vitro *Listeria* motility system with defined composition (*11*). *Arabidopsis* ADF1 increases the dissociation rate at the filament pointed (minus) end and was reported to enhance the association rate at the barbed (plus) end (*10*), although this latter point is controversial and may depend on whether severing of filaments took place (*12*). Furthermore, AC proteins are required for the generation of free barbed ends of actin at the leading edge of stimulated adenocarcinoma cells (reviewed in ref *12*) and for polarized migration of fibroblasts (*13*).

A structural basis for the enhancement of filament turnover by AC was proposed by McGough et al. (*14*), who found that AC proteins bind to a twisted form of actin that might have weaker longitudinal interactions. Galkin et al. (*15*) identified the twisted form of actin as a minor component of normal actin filaments, suggesting that AC proteins might bind selectively to this conformer and stabilize it.

Single-cell eukaryotes express only one member of the AC family, whereas metazoans express two or more members. Within and between any vertebrate species, ADF and cofilin have about 70% amino acid sequence identity. In addition, they share qualitative similarities in biochemical properties. They bind monomeric actin in a 1:1 complex and inhibit nucleotide exchange (*16*−*18*). Many AC proteins are reported to bind to ADP−G-actin with 30- to 80-fold higher affinity than they bind to ATP−G-actin at physiological ionic strength (*10*, *19*, *20*). The actin depolymerizing activity of many AC proteins is inhibited by their binding of PtdIns-(4,5)P_2 (*21*), at pHs below 7.1 (*16*, *18*), and by saturation of F-actin with some isoforms of tropomyosin (*22*, *23*) but perhaps not all of them (*24*). With the exception of the AC proteins from yeast and *Dictyostelium*, the activity of AC is inhibited by phosphorylation at ser3 (*25*) or its equivalent ser6 in plant ADF (*26*) or ser2 in amoeba actophorin (*27*). LIM kinases (*28*−*32*) and the related TES kinases (*33*−*35*) phosphorylate AC. Dephosphorylation of phosphorylated AC can be accomplished by ubiquitous phosphatases (reviewed

† This work was supported by National Institutes of Health grants GM35126 and GM54004 to J.R.B.

* To whom correspondence should be addressed. Tel.: (970) 491-6096. Fax: (970) 491-0494. E-mail: jbamburg@lamar.colostate.edu.

‡ Present address: Department of Biological Chemistry, Johns Hopkins University School of Medicine, Baltimore, MD 20205.

[1] Abbreviations used: ADF, actin depolymerizing factor; AC, ADF/cofilin; XAC, *Xenopus* AC.; tsr, twinstar gene product or *Drosophila* AC; Aip1, actin interacting protein 1; Cc, critical concentration; DBP, vitamin D binding protein (also called group-specific component); EM, electron microscopy; G-actin, monomeric or globular actin; F-actin, filamentous actin; PAGE, polyacrylamide gel electrophoresis; PtdIns-(4,5)P_2, phosphatidylinositol-4,5-bisphosphate.

10.1021/bi049797n CCC: $27.50 © 2004 American Chemical Society
Published on Web 05/07/2004

in ref *1*) but is likely to be more highly regulated in vivo through binding of the phosphorylated species by 14-3-3 ζ (*36*−*38*) and by the activity of specific phosphatases, particularly those of the slingshot family (*39*, *40*; reviewed in ref *41*).

Not all AC homologues show pH dependence. Chick ADF (*16*) and human ADF (*18*) have a pH-sensitive actin depolymerizing activity, but actophorin does not (*42*). Human ADF showed greater pH dependence than *Arabidopsis* ADF1 (*20*). Shifting to higher intracellular pH in mammalian cells expressing both ADF and cofilin resulted in greater co-localization of ADF with G-actin and reduced co-localization with F-actin, whereas the distribution of cofilin, which co-localized more with F-actin, was unchanged by pH shift (*43*).

ADF and cofilins are separate gene products that appear to have evolved from a single ancestral protein. The three distinct vertebrate subclasses, named ADF (also called destrin), nonmuscle cofilin (cof-1), and muscle cofilin (cof-2), emerged before the divergence of birds and mammals (*44*). In single-cell organisms, such as yeast, that express only one member of the AC family, functional defects in cofilin are lethal, but mutant yeast can be rescued with either mammalian ADF or nonmuscle cofilin (*4*, *45*). These results demonstrate that the two mammalian AC proteins have sufficient functional overlap to provide the regulation needed for actin dynamics in yeast.

Differences between the activities of members of the AC family within a single organism have been reported. In *Caenorhabditis elegans*, the ubiquitous unc60A has a much stronger filament severing and dynamizing activity than the muscle-specific unc60B (*46*), which is presumably more closely related to cof-2 in mammals. Indeed, mouse cof-2 is the weakest of the three mammalian isoforms in its ability to sever and depolymerize actin filaments (*47*). The ADF and cofilin-1 from human (*48*) and mouse (*47*) appear to be much more similar in their effects on actin dynamics, with only some minor differences in quantitative binding being observed.

This study investigates the interaction of chick ADF and chick cofilin with G- and F-actin using assays that allow us to determine quantitative differences in their interactions. It differs from other studies in that we purify and characterize the recombinant proteins using similar methods and utilize a few novel assays, including a double-end-capping assay, to characterize their interactions with actin. Here, we demonstrate that there are differences between chick ADF and chick cofilin in G-actin binding, filament severing, off-rate enhancement, and pH sensitivity. Furthermore, comparative assays with similarly prepared recombinant AC proteins from across the eukaryotic phyla show that they fall into two major subclasses. Members of the ADF group are more effective in filament depolymerization (which includes severing, off-rate enhancement, and monomer sequestering) than are the members of the cofilin group. Unlike ADF, members of the cofilin group promote filament assembly by severing without substantially increasing the critical concentration. These findings help explain previously reported comparative activities as well as behavioral and morphological differences that have been observed in cells in which either an ADF or a cofilin has been overexpressed. They might also help explain the requirement for the coexpression of both constitutively active forms of ADF and cofilin to obtain an effect on *Salmonella* invasion of mammalian cells, whereas expression of either active mutant by itself has no effect (*49*).

EXPERIMENTAL PROCEDURES

Proteins. Ca^{2+}−ATP−G-actin was extracted from chick muscle acetone powder and purified according to Pardee and Spudich (*50*). G-Actin was gel filtered over Sephadex G-150 in G-buffer (2 mM Tris, 0.2 mM ATP, 0.5 mM DTT, 0.2 mM $CaCl_2$, 0.01% NaN_3, pH 8.0), and the final ATP was adjusted to 0.5 mM prior to freezing 100 μL aliquots in liquid N_2. Mg^{2+}−ATP−G-actin was prepared from Ca^{2+}−ATP−G-actin by incubation with 0.1 mM $MgCl_2$ and 0.2 mM EGTA for 10 min on ice (*51*). The Mg^{2+}−ATP−G-actin was converted to Mg^{2+}−ADP−actin by the addition of 1 mM glucose and 20 U/mL hexokinase and incubation for 1 h (*52*).

Chick brain ADF was purified from frozen 14- to 17-day-old embryonic chick brain (*53*). Recombinant chick ADF and chick cofilin were prepared as described by Adams et al. (*54*) and Abe et al. (*55*, *56*), respectively. Both ADF and cofilin were bound to and eluted from a Green A column (Millipore) as the final step of purification. ADF was bound to a Green A column in 10 mM Tris, pH 7.5, and 5 mM DTT; cofilin was bound to a Green A column in 10 mM PIPES, 10 mM Tris, pH 6.5, and 5 mM DTT. Both ADF and cofilin were eluted with salt gradients up to 200 mM NaCl in the respective buffer.

Recombinant human ADF was prepared as described by Hawkins et al. (*18*). As a final step, the human ADF was bound and eluted from Green A−agarose as described for chick ADF (*53*). Recombinant *Xenopus* XAC was prepared as described by Abe et al. (*7*). XAC1 and XAC2 were cleaved from GST fusion proteins with thrombin. Recombinant *Drosophila* ADF/cofilin (product of the twinstar gene) was expressed in *Escherichia coli* strain BL21pLysS and purified by chromatography on DEAE−cellulose and Green A resin, similar to the purification scheme for recombinant chick ADF (*54*) but with the pH of the Green A-binding buffer reduced to pH 7.5 at 4 °C. Recombinant *Arabidopsis* ADF1 was expressed in *E. coli* strain BL21DE3 as a GST-ADF1 fusion protein, purified on a glutathione column, and cleaved by thrombin. *Acanthamoeba* actophorin, *Saccharomyces* cofilin, starfish depactin, *Dictyostelium* cofilin, and *C. elegans* UNC-60A and UNC-60B were kindly provided by Drs. Blanchoin, Drubin, Mabuchi, Condeelis, and Ono, respectively.

All AC proteins were dialyzed against 2 mM Tris, pH 8.4, containing 0.5 mM DTT before incubation with actin in studies using non-denaturing polyacrylamide gel electrophoresis (PAGE). The purity of proteins was determined using SDS−PAGE. The concentration of G-actin was determined spectrophotometrically using the extinction coefficient of 0.63 L/g at 290 nm (*57*). The extinction coefficients at 280 nm are 11 650 M^{-1} cm^{-1} for chick ADF, 18 020 M^{-1} cm^{-1} for chick cofilin, 19 540 M^{-1} cm^{-1} for *Xenopus* XAC1, 16 530 M^{-1} cm^{-1} for *Drosophila* ADF/cofilin (tsr), 12 690 M^{-1} cm^{-1} for *Arabidopsis* ADF1, 12 530 M^{-1} cm^{-1} for *Acanthamoeba* actophorin, and 8040 M^{-1} cm^{-1} for *Caenorhabditis* UNC-60A and UNC-60B, all calculated by the method of Gill and von Hippel (*58*), which was developed for denatured proteins. The concentrations of AC proteins

were first calculated by spectrophotometric measurement in G-buffer and then checked by quantification on Coomassie Blue R-250-stained SDS−polyacrylamide gels using actin for generating a standard curve. AC concentrations determined by this method were within 10% of the value determined spectrophotometrically.

Recombinant human gelsolin was prepared as described by Pope et al. (*59*). The extinction coefficient for gelsolin at 280 nm is 114 230 M^{-1} cm^{-1} (*59*). Gelsolin−actin 1:1 complex was prepared by mixing equal molar amounts of gelsolin and G-actin in the presence of 10 mM $CaCl_2$ and incubating for 10 min prior to adding 30 mM EGTA. The complex was gel-filtered over Sephadex G-150 in 10 mM HEPES, pH 7.0, 50 μM $MgCl_2$, 0.1 mM EGTA, 1 mM NaN_3, and 0.2 mM DTT (*60*). Because the peak of free gelsolin overlaps the peak of the complex, care must be taken to exclude any fractions containing free gelsolin as determined by non-denaturing gel electrophoresis (bicine−triethanolamine system described below) of the column fractions. Human vitamin D-binding protein (DBP), also called Gc-globulin, was purchased from Calbiochem-Novabiochem Co. (La Jolla, CA). Spectrin:actin:protein 4.1 complex was kindly provided by Drs. James Casella and Susan Craig (Johns Hopkins University).

Non-denaturing Polyacrylamide Gel Electrophoresis. Non-denaturing polyacrylamide gel electrophoresis was used to study the effect of actin-bound nucleotide and divalent cation on the interaction between AC protein and G-actin. The AC at concentrations from 0 to 10 μM was mixed with G-actin in 2 mM Tris, pH 8.4, and 0.5 mM DTT containing either 0.2 mM ATP or ADP. The mixtures were incubated for 15 min at room temperature, and the free actin and the complex of actin-AC protein were then separated on a 7.5% non-denaturing polyacrylamide gel at 4 °C. The 1× running buffer contained 50 mM bicine, 40 mM triethanolamine, pH 8.4, 0.2 mM ATP or ADP, and, if assaying for the interaction with Mg−actin, 5 mM EGTA, at an ionic strength of 34 microsiemens (μS). The concentration of bicine and triethanolamine in the running buffer was varied from 0.5× to 3× to adjust the ionic strength from 20 to 90 μS. Gels were stained with Coomassie Blue R-250 when aliquots from samples containing 5 μM G-actin were used, and stained with SYPRO red (Molecular Probes) when aliquots from samples containing 1.5 μM G-actin were used. An internal actin standard was run on each gel to normalize the staining so that standard curves run on other gels could be used to quantify the concentration of free actin and AC−actin complex. Digitized images were obtained with a Photometrics chilled CCD camera, and band densities were quantified using 1D Phoretix software (Non Linear Dynamics Ltd, England) and analyzed by KaleidaGraph analysis/graphics software (Synergy Software, Reading, PA). An estimate of the apparent dissociation constant (K_D) defined in eq 1 was obtained by curve fitting to the transformed form of eq 1 shown as eq 2.

$$K_{D\,app} = \frac{[\text{actin}]_f[\text{AC}]_f}{[\text{AC}-\text{actin}]} \quad (1)$$

$$[\text{AC}-\text{actin}] = ([\text{AC}]_t + K_D + A)/2 - \{[\text{AC}]_t[\text{AC}]_t + 2(K_D - A)[\text{AC}]_t + (K_D + A)(K_D + A)\}^{0.5}/2 \quad (2)$$

In these equations, $[\text{actin}]_f$ is the concentration of free actin measured directly from the gel; $[\text{AC}]_f$ is the concentration of free ADF or cofilin and was estimated as the difference between the total AC and the amount of AC in the AC−actin complex; [AC−actin] is the concentration of AC−actin complex measured directly from the gel; $[\text{AC}]_t$ is the total concentration of ADF/cofilin. *A* is the total concentration of actin, 5 μM for Coomassie-stained gel and 1.5 μM for SYPRO red-stained gel. In entering eq 2 into Kaleidagraph, the following substitutions are made: $m0 = [\text{AC}]_t$; $m1 = K_D$. Since this is not a true equilibrium system, measurements are reported only as $K_{D\,app}$.

The amount of actin displaced by DBP from ADF−actin 1:1 complex was also measured by non-denaturing gel electrophoresis. To form this complex, 5 μM MgATP−actin and 15 μM ADF were incubated in 2 mM Tris, pH 8.4, 0.5 mM DTT, 0.2 mM ATP, 0.21 mM $MgCl_2$, and 0.2 mM EGTA for 10 min on ice. A 3:1 ADF-to-actin ratio was used to drive most of the actin into complex. Increasing concentrations of DBP were incubated with the ADF−actin complex for 15 min at room temperature. The proteins were separated on a 7.5% non-denaturing polyacrylamide gel at 4 °C using 50 mM bicine, 40 mM triethanolamine, 0.2 mM ATP, pH 8.4, as the running buffer. The gel was stained with Coomassie Blue R250. Digitized gel images were obtained and analyzed as above.

Job Plot. Because ADF/cofilins bind to G-actin in a 1:1 molar ratio as determined by gel filtration and chemical cross-linking (*17*, *53*), a Job plot (*61*) was used to determine if the different AC preparations and actin were equally active and homogeneous in binding affinity. In this method, the total molar concentration of AC and either Ca^{2+}−ATP−actin or Ca^{2+}−ADP−actin was held constant and the mole fraction of each was varied. Ca^{2+}−ATP−actin was used in the interaction with chick ADF and XAC1, and CaADP−actin was used in the interaction with chick cofilin, *Drospohila* AC, actophorin, *Arabidopsis* ADF1, UNC 60A, UNC 60B, and human ADF. The mixtures were then subjected to non-denaturing polyacrylamide gel electrophoresis to separate free actin and AC−actin complex. The concentration of complex was plotted against the molar ratio of ADF or cofilin to actin. If recombinant protein preparations contain >20% of inactive protein, the position of the peak will deviate substantially from its position at a 1:1 molar ratio. No such deviations were observed.

Timed Sedimentation Assay. The steady-state filament length distribution in the presence of AC protein was studied by a timed sedimentation assay. Actin at 20 μM was polymerized alone or in the presence of 20 μM AC in pH 8.1 F-buffer (final concentrations of 0.1 M KCl, 2 mM $MgCl_2$, 1 mM DTT, 0.2 mM ATP, 0.2 mM EGTA, 15 mM Tris, 15 mM PIPES, with a calculated ionic strength of 130 μS) containing an ATP-regenerating system (10 U/mL creatine phosphokinase and 10 mM creatine phosphate). The samples were incubated at 4 °C overnight and then centrifuged at 4 °C from 5 min to 60 min at 436000*g* in the Beckman TLA100 rotor. The total supernatant was removed and mixed to ensure uniform sampling, and the pellet was resuspended in SDS-containing buffer (0.25 M Tris, pH 6.8, 10% glycerol, 10% β-mercaptoethanol, and 1% SDS). Fractions from supernatant and pellet were subjected to SDS−PAGE (15% T, 2.67% C).

SDS−PAGE. Samples with unknown protein concentration and five actin standards (0.1−1.6 μg) were loaded on an 18-well SDS−polyacrylamide mini gel (15% T, 2.67% C) (*62*). After electrophoresis, the gel was stained with Coomassie Blue R-250. The gel image was digitized using a CCD camera, and bands were quantified using the 1D Phoretix program (Synergy Software). The amount of protein in each sample was obtained from the actin standard curve, which was determined to be in the linear range for analysis.

Electron Microscopy. Aliquots from samples used for nondenaturing PAGE were also used for electron microscopy. G-Actin and ADF or cofilin were mixed in 2 mM Tris, 0.5 mM DTT, 0.2 mM ATP, 50 mM Bicine, 40 mM triethanolamine, and 5 mM EGTA, pH 8.4, at room temperature for 30 min. Aliquots (10 μL) of the mixtures were applied to 0.5% Formvar-coated copper grids. After 15 s, filaments adhering to the grid were negatively stained by applying 5 drops of 1% uranyl acetate and blotting off the excess. Grids were examined in a JEOL electron microscope at 100 kV.

Aliquots of the total sample and supernatants from a timed sedimentation assay were fixed with 0.1% glutaraldehyde and diluted with water to give a concentration of actin of about 1 μM. A 2 μL aliquot of the diluted sample was applied to a Formvar-coated copper grid, air-dried to adhere all filaments, and negatively stained as described above.

Filament Severing Assay. Filament severing by different AC proteins was measured by the relative depolymerization rates from newly generated pointed ends. In this assay, 60 nM spectrin:actin:protein 4.1 complex (only about 3.1% active as measured by nucleated filament elongation rate assays) and 3.3 μM actin (5% pyrene-labeled) were mixed in pH 6.8 F-buffer (100 mM KCl, 2 mM $MgCl_2$, 0.2 mM ATP, 0.2 mM EGTA, 0.5 mM DTT, and 10 mM PIPES) or pH 7.8 F-buffer (same salts but with 10 mM Tris instead of PIPES; both buffers passed through 0.2 μm filters and degassed) to nucleate filament growth from the barbed ends. Changes in fluorescence intensity were monitored at 18 °C with an AVIV ATF 105 spectrofluorometer set for excitation at 365 nm and emission at 404 nm. The bandwidth was 2 nm for excitation and 4 nm for emission. The steady state, as determined by the fluorescence signal reaching a plateau, was reached in 6 min (followed for up to 60 min in some experiments). Upon reaching steady state, 200 nM gelsolin−actin 1:1 complex and 0.6 μM AC protein were added, and the sample was incubated for 10 min. Gelsolin−actin 1:1 complex will cap free barbed ends including initial free barbed ends and those generated by severing. DBP, a potent actin monomer sequestering protein (K_D = 1 nM; ref *63*), was added in excess to sequester monomers and thus induce depolymerization from the pointed ends of the filaments by maintaining the actin concentration below the critical concentration.

Measurement of Filament Severing and Rates of Depolymerization at Pointed Ends. The rate of depolymerization from pointed ends was measured using a modification of the method of Moriyama and Yahara (*64*). Ca−G-actin (5% pyrenyl-labeled, 0.2 mM $CaCl_2$, 2 mM Tris, pH 8.0) was incubated with $MgCl_2$ (1 molar equiv and 50 μM in excess) on ice for 10 min and mixed with various concentrations of gelsolin for 10 min to form gelsolin−actin seeds, and then F-buffer either at pH 6.8 or pH 7.8 was added to initiate polymerization from the pointed ends. After 4 h of polymerization at room temperature, ADF or cofilin and gelsolin−actin 1:1 complex (77 nM at pH 6.8 or 154 nM at pH 7.8) were added and allowed to incubate at room temperature for 10 min. The gelsolin−actin 1:1 complex caps the free barbed ends generated by the severing action of ADF or cofilin. DBP was then added to induce depolymerization from the pointed ends of the filaments. Changes in fluorescence intensity were monitored at 18 °C with an AVIV ATF 105 spectrofluorometer. The dead time was about 10 s, and the final concentrations for actin and DBP were 3.34 and 3.5 μM, respectively. The wavelengths and bandwidths are the same as described above. The assay was also run without pyrene-labeled actin using light scattering at 400 nm to follow filament depolymerization.

The initial off-rate from pointed ends (V_i) is proportional to the total number of free pointed ends (N_p) and the pointed end off-rate constant (k_{p-}). The total number of free pointed ends, N_p, can be expressed as the summation of the initial number of filaments (N_o), taken to be identical to the gelsolin concentration used to nucleate filament growth, and the number of filaments created by ADF or cofilin severing (n):

$$V_i = k_{p-}N_p = k_{p-}(N_o + n)$$

Calibration of Nucleating Activity of Gelsolin and Spectrin:Actin:Protein 4.1 Complex. The concentration of spectrin:actin:protein 4.1 complex was determined from Coomassie-stained SDS polyacrylamide gels using actin as the standard. The activity of spectrin:actin:protein 4.1 complex was estimated from its ability to nucleate actin seeds for polymerization. In brief, various amounts of spectrin:actin:protein 4.1 complex were mixed with MgATP−G-actin (3.3 μM final concentration, 5% pyrenyl-labeled). Polymerization was initiated by adding concentrated salts and Tris to achieve pH 7.8 F-buffer conditions and was followed with an AVIV spectrofluorometer. The initial rate of polymerization (V_i) was obtained from the raw plot. The number of nucleation seeds (N) was derived from the equation $V_i = k^+_{on}[N][GA] - k^+_{off}[N]$. The concentration of G-actin ([GA]) is 3.3 μM, the plus end on-rate constant is 3.36 μM^{-1} s^{-1}, and the plus end off-rate constant is 0.32 s^{-1} (*65*). The amount of nucleation seeds was calculated to be 3.1% of total spectrin:actin:protein 4.1 complex.

The concentration of active gelsolin was calculated on the basis of its ability to nucleate actin seeds for polymerization from the minus ends. Ca−G-actin (5 μM final concentration, 5% pyrenyl-labeled) was incubated with $MgCl_2$ (1 molar equiv and 50 μM in excess) on ice for 10 min and then mixed with 25 nM gelsolin and incubated on ice for 10 min. Polymerization was initiated by adjusting to pH 7.8 F-buffer conditions with concentrated stocks and followed by fluorimetry. The initial rate of polymerization obtained from the raw plot was used to determine the number of nucleation seeds from the equation $V_i = k^-_{on}[N][GA] - k^-_{off}[N]$. The concentration of G-actin ([GA]) is 5 μM, the minus end on-rate constant is 0.26 μM^{-1} s^{-1}, and the minus end off-rate constant is 0.27 s^{-1} (*65*). The amount of nucleation seeds was calculated to be 8.5% of total gelsolin.

Measurement of Critical Concentration. Actin at 16 μM was polymerized for 5 h in pH 7.8 F-buffer in the absence or in the presence of ADF or cofilin. ADF and cofilin were in 2.5 molar ratio to actin. The samples were then diluted

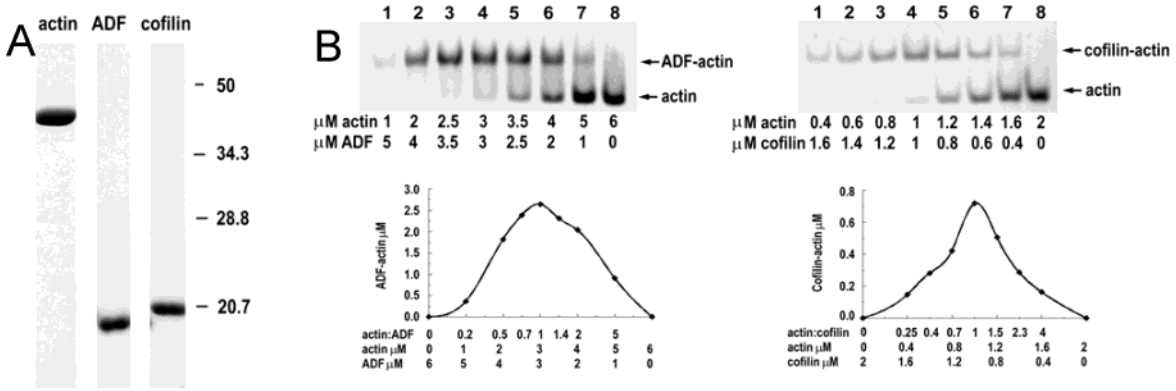

FIGURE 1: Purity and actin binding stoichiometry of representative ADF/cofilin proteins. (A) SDS−PAGE of purified actin (1.6 μg), chick ADF (1 μg), and chick cofilin (1 μg). The 15% gel was stained with Coomassie Blue R-250. Positions of molecular mass markers (kD) are shown. (B) Job plots of the complex formed between chick ADF and chick cofilin and actin on non-denaturing gels. Gels show complex formed between actin and chick ADF (left) or chick cofilin (right), using constant total protein and varying the ratios. For ADF the total protein was held at 6 μM, whereas for cofilin the total protein was kept at 2 μM, because cofilin induced assembly at higher concentrations (see Figure 3 and Results). Job plots of the scanned gels showing peak of complex formed at a 1:1 ratio of the AC protein to actin for ADF and cofilin. Similar results were obtained for *Xenopus* ADF/cofilin (XAC1), *Drosophila* ADF/cofilin (tsr), *Acanthamoeba* actophorin, *Arabidopsis* ADF1, *C. elegans* UNC60A and UNC60B, and *Homosapien* ADF.

with pH 7.8 F-buffer to final actin concentrations from 2 to 14 μM. The light scattering signals of the steady-state F-actin were monitored at 17 °C with an AVIV ATF 105 spectrofluorometer at 400 nm. The signal is plotted against actin concentration, and the critical concentration is derived from the intercept by linear regression.

RESULTS

Characterization of the Proteins for Purity and Homogeneous Binding Activity. The purity of actin and AC proteins used here was determined by densitometric scanning of Coomassie Blue R-250-stained SDS−polyacrylamide gels (Figure 1 and data not shown). The purity was estimated to be 87% for human ADF, 97% for XAC1, 94% for XAC2, and >98% for the other AC proteins and actin. Job plots of AC binding to G-actin were used before each experiment to verify that each protein was active and homogeneous with respect to actin binding. The maximum formation of the AC−actin complex was reached at a 1:1 molar ratio of AC to actin (Figure 1 and Supporting Information Figure 1) for each of AC proteins tested. Since ACs bind to G-actin in a 1:1 molar ratio (*17*, *53*), our preparations of ACs and actin do not contain a significant fraction of inactive protein. We were unable to demonstrate a complex between G-actin and either yeast cofilin or *Toxoplasma gondii* ADF by non-denaturing gel electrophoresis, either because the complex migrated identically to free actin or because binding was too weak to measure.

Effect of Actin-Bound Nucleotide and Divalent Metal on the Interaction between G-Actin and Chick ADF or Chick Cofilin. Non-denaturing PAGE was used to determine the apparent dissociation constants of chick ADF−G-actin and chick cofilin−G-actin. Under the normal low ionic strength (34 μS) conditions used for electrophoresis, ADF had slightly weaker apparent affinity for Mg^{2+}−ATP−G-actin than for Mg^{2+}−ADP−G-actin (~2-fold difference in $K_{D\,app}$), and the binding was not substantially affected by the bound cation (Ca^{2+} vs Mg^{2+}) (Figure 2; Table 1). However, the interaction of cofilin with actin was very dependent upon both the divalent metal and the bound nucleotide. Cofilin bound equally well to the Ca^{2+}−ATP, Ca^{2+}−ADP, and Mg^{2+}−ADP forms of actin (Figure 3d−f; Table 1). However, cofilin formed only trace amounts of complex when mixed with 5 μM Mg^{2+}−ATP−actin (Figure 3b), although the free actin disappeared from the gel as cofilin levels increased. This observation suggested either that cofilin−actin had a lower critical concentration for assembly or that nucleated assembly was better than actin alone and thus induced filament formation even at the relatively low (34 μS) ionic strength of the running buffer. We repeated the binding study between cofilin and Mg^{2+}−ATP−actin using a lower concentration of actin (1.5 μM) and the more sensitive, but linearly responsive protein stain SYPRO red to detect the lower amounts of protein. Under these conditions, the total actin (free actin and the cofilin−actin complex) was fully recovered in the gel (Figure 3g,h). Cofilin binds to Mg^{2+}−ADP−actin with about 20× higher apparent affinity than to Mg^{2+}−ATP−actin (Figure 3i; Table 1). Thus, chick ADF and cofilin show similar high apparent affinity binding for Ca^{2+}−ATP−actin, Ca^{2+}−ADP−actin, and Mg^{2+}−ADP−actin, but only chick cofilin shows a marked decrease in affinity for Mg^{2+}−ATP−actin.

Effect of Ionic Strength on the Interaction between G-Actin and Chick ADF or Chick Cofilin. We varied the ionic strength of the running buffer for the non-denaturing gels from 20 to 90 μS (0.5× to 3× running buffer). Consistent with previous observations (*10*), apparent affinities of ADF for Mg^{2+}−ATP−actin and Mg^{2+}−ADP−actin decreased in parallel about 40-fold with increasing ionic strength (Table 2). At the highest ionic strength (90 μS) at which the gels could be run, chick cofilin bound to Mg^{2+}−ADP−actin with about a 3-fold higher apparent affinity than chick ADF. At this ionic strength, no cofilin−actin complex was detected by Coomassie blue staining when 5 μM Mg^{2+}−ATP−actin and increasing amounts of cofilin were used, and the free actin disappeared from the gel, again suggesting cofilin induced actin filament assembly.

Cofilin Promotes F-Actin Assembly. To determine if the disappearance of the actin from the gels in the presence of cofilin was due to filament assembly, aliquots of the samples prepared for non-denaturing gel electrophoresis were applied to EM grids, negatively stained, and observed in the electron

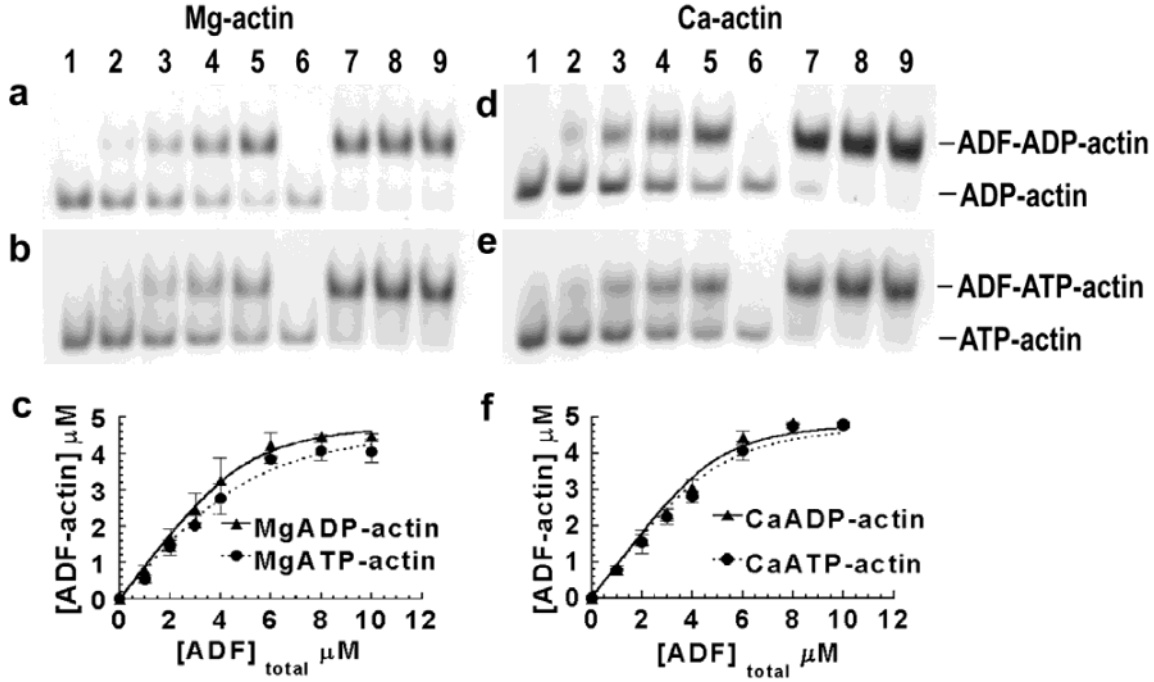

FIGURE 2: Interaction of ADF with G-actin is not greatly affected by the nucleotide or divalent cation bound to actin. Chick ADF (0, 1, 2, 3, 4, 6, 8, and 10 μM; lanes 1, 2, 3, 4, 5, 7, 8, and 9, respectively) was incubated with (a) 5 μM MgADP−actin, (b) 5 μM MgATP−actin, (d) 5 μM CaADP−actin, or (e) 5 μM CaATP−actin. An internal standard of 2.5 μM actin was loaded in lane 6. Each lane was loaded with 12 μL of sample. The complex was separated from free actin by non-denaturing PAGE and stained with Coomassie Blue R. The binding curves were obtained by quantitative densitometry of gels. The amount of complex was plotted against the amount of total ADF, as shown in panel c for the interaction with Mg−actin and in panel f for the interaction with Ca−actin. The curves were fitted to the equation (see Materials and Methods) to obtain the apparent dissociation constants.

Table 1: $K_{D\,app}$ of ADF/Cofilins for G-Actin at Ionic Strength 34 μS As Determined by Measuring Complex Following Non-denaturing Polyacrylamide Gel Electrophoresis

	$K_{D\,app}$ (μM)[a]			
	MgATP−actin	MgADP−actin	CaATP−actin	CaADP−actin
chick ADF	1.0 (4)	0.5 (4)	0.5 (3)	0.4 (3)
chick cofilin	18 (3)	0.6 (3)	0.9 (3)	0.7 (3)
chick cofilin	10.7[b] (3)	0.5[b] (3)		
Xenopus XAC1	0.8 (4)	0.4 (3)	0.5 (3)	0.6 (3)
Drosophila AC	21 (4)	0.5 (4)	1.0 (3)	0.5 (3)
plant ADF	nm[c] (1)	1.1 (1)	0.73 (1)	0.49 (1)
UNC 60B	>16 (1)	2.8 (1)	3.8 (1)	1.4 (1)
Actophorin	nm (3)	3.1 (3)	nm (3)	nm (3)

[a] The number in the parentheses indicates the number of experiments. [b] SYPRO red staining with 1.5 μM actin. All others measured with 5 μM actin. [c] nm, no measurable AC−actin complex ($K_{D\,app}$ > 25 μM).

microscope. Under the standard gel electrophoresis buffer conditions (34 μS and pH 8.4), no filaments were observed in the samples of 5 μM actin alone or of 5 μM actin and 2 μM ADF, even after 30 min of incubation (Figure 4a,b). However, many filaments were observed in samples containing 5 μM Mg^{2+}−ATP−actin and 2 μM cofilin (Figure 4c). These data demonstrate that cofilin, but not ADF, promotes actin filament assembly at these concentrations and under relatively low ionic strength. The enhanced filament assembly in the presence of cofilin could arise from cofilin being able to (1) decrease the critical concentration for assembly (i.e., assembly of cofilin−actin complex), (2) enhance nucleation, (3) inhibit actin dissociation from filament plus ends, or (4) enhance the assembly rate constant at the plus end. These possibilities are examined below.

One of the possible reasons for cofilin to be able to induce filament assembly, under conditions where actin alone or in the presence of ADF did not assemble, is to reduce the critical concentration for assembly. Therefore, we measured the critical concentration for assembly using a light scattering assay to quantify relative polymer mass, and we performed the assay at a 2.5:1 molar ratio of ADF or cofilin to actin at near physiological ionic strength at pH 7.8 (Figure 5). The substantially different slopes between the samples of actin alone and those with ADF or cofilin reflect the greater light scattering of the ADF or cofilin−actin copolymer (*10*). The critical concentration (intercept on abscissa) of chick cofilin−actin (0.8 μM) is much lower than that of chick ADF−actin (6.2 μM) but still higher than that of actin alone (0.2 μM). Thus, the promotion of filament assembly by cofilin cannot simply be explained by an alteration in the critical concentration. Cofilin must act through a more complicated mechanism. As shown below, this includes enhancing nucleation of filaments.

ADF Enhances Filament Numbers Compared to Cofilin. A timed sedimentation assay was performed in pH 8.1 F-buffer with 20 μM actin to estimate the steady-state distribution of filament lengths in mixtures of actin incubated with either chick ADF or chick cofilin. Because we incubated the samples overnight to achieve a true steady state, we included an ATP-regenerating system in the mixture to maintain ATP levels. After centrifugation for 5 min at 436000*g*, 85% of the actin pelleted in samples containing actin alone and 75% pelleted in samples containing actin and chick cofilin in a 1:1 molar ratio (Figure 6a,b). In the presence of chick ADF, less than 50% of the actin sedimented within 5 min, and it took 35 min to sediment 75%

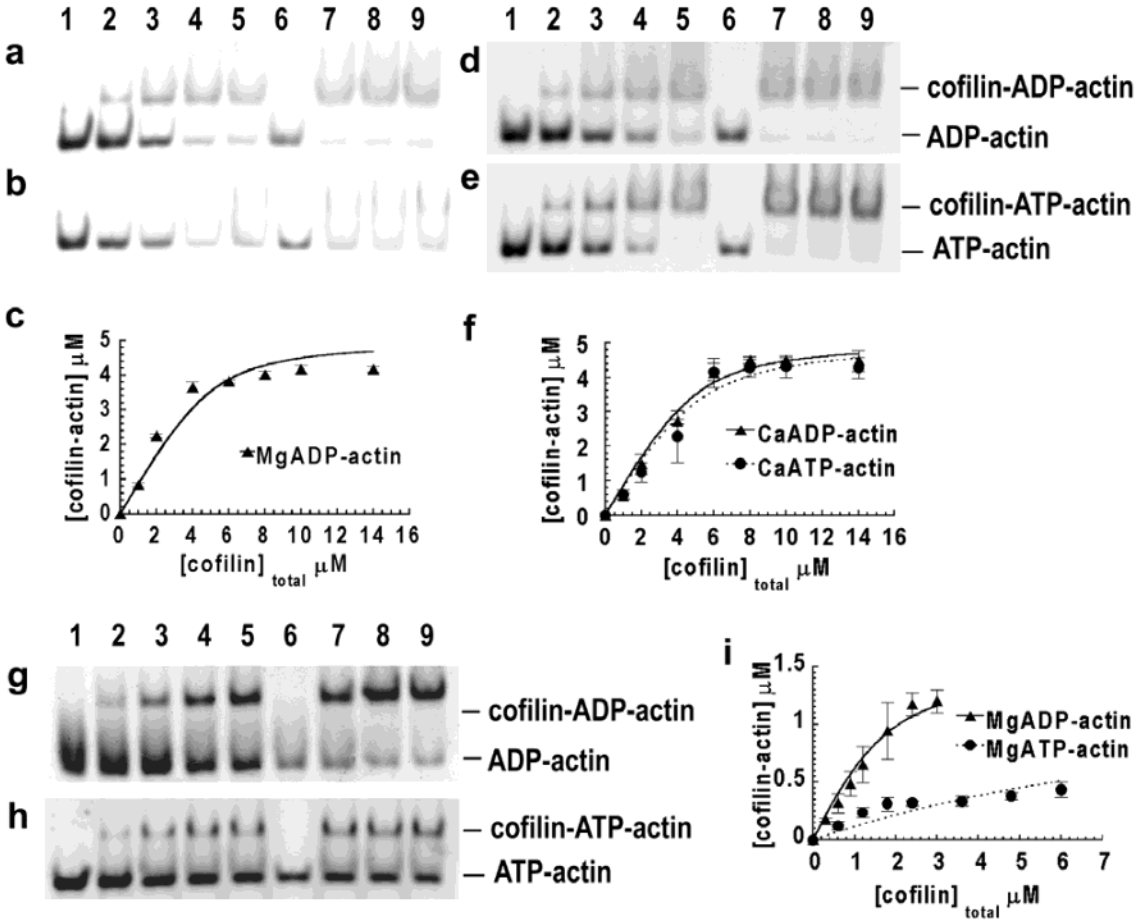

FIGURE 3: Interaction of cofilin with G-actin is affected by the nucleotide and divalent cation bound to the actin. Chick cofilin (0, 1, 2, 4, 6, 8, 10, and 14 μM; lanes 1, 2, 3, 4, 5, 7, 8, and 9, respectively) was incubated with (a) 5 μM MgADP−actin, (b) 5 μM MgATP−actin, (d) 5 μM CaADP−actin, or (e) 5 μM CaATP−actin. (g) Chick cofilin (0, 0.3, 0.6, 0.9, 1.2, 1.8, 2.4, and 3 μM; lanes 1, 2, 3, 4, 5, 7, 8, and 9, respectively) was incubated with 1.5 μM MgADP−actin. (h) Chick cofilin (0, 0.6, 1.2, 1.8, 2.4, 3.6, 4.8, and 6 μM; lanes 1, 2, 3, 4, 5, 7, 8, and 9, respectively) was incubated with 1.5 μM MgATP−actin. An internal standard of 2.5 μM actin (a, b, d, and e) or 0.75 μM actin (g and h) was used in lane 6. Each lane was loaded with 12 μL of sample. The complex was separated from free actin on non-denaturing PAGE. Gels in panels g and h were stained with SYPRO red, and gels in panels a, b, d, and e were stained with Coomassie Blue R-250. Binding curves obtained by quantitative densitometry of gels are shown in panels c and i for Mg−actin and in panel f for Ca−actin. The curves were fit to eq 2 (see Materials and Methods) to give apparent dissociation constants.

Table 2: $K_{D\,app}$ of Chick ADF and Chick Cofilin for G-Actin at Ionic Strength, 20−90 μS, As Determined by Measuring Complex Following Non-denaturing Polyacrylamide Gel Electrophoresis

	$K_{D\,app}$ (μM)[a]			
	chick ADF		chick cofilin	
ionic strength (μS)	MgATP−actin	MgADP−actin	MgATP−actin	MgADP−actin
20	0.28 (4)	0.08 (4)		
34	1.0 (4)	0.5 (4)	10.7[b] (3)	0.5[b] (3)
62	1.3 (3)	0.29 (3)		
90	12.4 (3)	3.2 (3)	>40 (3)	1.1 (3)

[a] Number in parentheses indicates number of replicate experiments. [b] SYPRO red staining.

(Figure 6a,b). To determine the approximate sizes of filaments sedimenting at the different times, we calculated the clearance times using the equation $t = k/s$, where t is the clearance time in hours, k is the clearance factor for the rotor (7 for Beckman TLA operating at 436000g), and s is the sedimentation coefficient of the filament in Svedberg units (Sv). The sedimentation coefficients were calculated assuming the actin filaments are rigid rods (*66*, *67*), although this is not the case with long filaments. Actin filaments containing more than 35 subunits (96 nm in length) should sediment within 5 min, whereas a tetrameric globular complex of two actin subunits and two molecules of ADF or cofilin (approximately 12 Sv) should sediment in 35 min. An actin dimer (approximately 7.6 Sv) will not be cleared until about 55 min. Our data suggest that long filaments predominate in solutions containing either F-actin alone or F-actin with chick cofilin and that a shorter, but more heterogeneous filament population predominates in F-actin solutions containing chick ADF.

The length distribution of filaments present initially in the timed sedimentation experiment was determined by measurements of negatively stained filaments from sample aliquots applied to Formvar-coated EM grids. Long and straight filaments were observed in samples of F-actin alone (Figure 6c), long and curved filaments predominate in cofilin−actin mixtures (Figure 6e), whereas short filaments predominate in ADF−actin mixtures (Figure 6d). Both filament distributions fit an exponential where the mean and median filament lengths are, respectively, 575 and 391 nm in the cofilin−actin mixture and 291 and 89 nm in the ADF−actin mixture (Figure 6f). The ratio of the median to the mean of 0.3 fits the expectation of a random severing distribution for ADF,

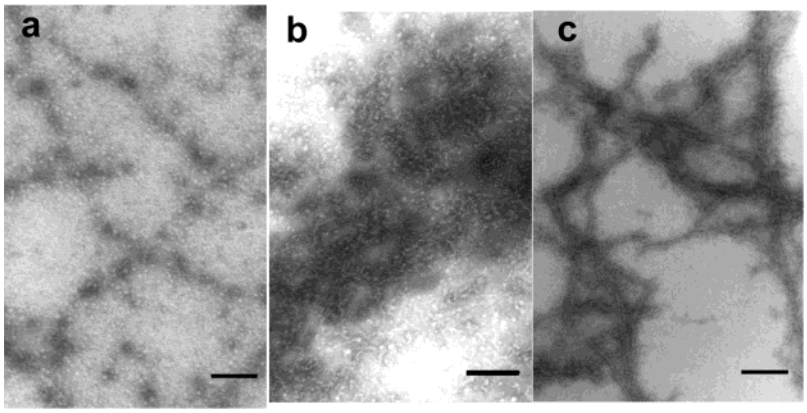

FIGURE 4: Cofilin promotes filament assembly. Samples prepared for electrophoresis on non-denaturing gels were incubated for 30 min, and aliquots were negatively stained and viewed by electron microscopy. No filaments were found in the samples containing 5 μM actin alone (a) or in the presence of 2 μM ADF (b). However, numerous actin filaments were observed in samples containing 5 μM actin and 2 μM cofilin (c) under the same conditions. Bars, 200 nm.

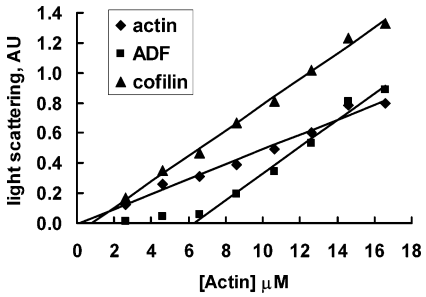

FIGURE 5: Cofilin−actin has a lower critical concentration than ADF−actin. Actin (2−16 μM) was polymerized in pH 7.8 F-buffer either in the absence or in the presence of a 2.5 molar excess of chick cofilin or chick ADF. The light scattering signals of the samples at steady state were plotted against actin concentration, and the intercepts, determined from least-squares linear regression analysis, represent the critical concentration.

but the value of 0.68 for the median/mean ratio for cofilin suggests that other factors, such as altered nucleation of new filaments, could contribute to the final distribution observed (*68*). To help distinguish between these possibilities, we developed an assay that is dependent upon filament severing to measure depolymerization rates from pointed ends.

ADF Is More Effective Than Cofilin in Filament Severing/Depolymerization and Is More pH-Dependent. A severing assay was developed in which actin (3.3 μM containing 5% pyrene label) was nucleated with 60 nM spectrin:actin:protein 4.1 complex at the pointed end, and, after steady state was reached, the barbed end was capped by gelsolin:actin 1:1 complex (present in excess). In contrast to the previous double-end-capped assay (*23*), the depolymerization rate was measured following addition of DBP to sequester actin monomer in the presence or in the absence of ADF or cofilin at pH 7.8 and pH 6.8 (Figure 7). F-Actin treated with ADF or cofilin buffer gave almost no change in assembly as measured by loss of pyrene fluorescence, demonstrating that filament ends are blocked. The slight decline observed in fluorescence in some samples probably arises from the slight mechanical severing in transferring the sample to the cuvette, which was minimized by using cut tips. Filaments treated with either 0.6 μM ADF or cofilin showed enhanced depolymerization compared to actin controls treated identically with buffer (Figure 7). The initial depolymerization rates in the presence of ADF relative to actin alone are 22 at pH 7.8 and 11 at pH 6.8, whereas rates in the presence of cofilin relative to actin alone are 3 at pH 7.8 and 4 at pH 6.8 (Table 3). These findings demonstrate that both ADF and cofilin sever filaments at both pHs, but that ADF is more pH-dependent than cofilin. However, because the depolymerization rate is a product of the number of pointed ends (severing) and the subunit off-rate, this assay cannot determine the relative importance of each of these two processes, or if one or the other predominates at the different pHs. Furthermore, the assay is biased toward severing, since even large pH-dependent increases in off-rate could not be detected in the absence of severing. Therefore, we utilized a method developed by Moriyama and Yahara (*64*) that permits measurements of severing and changes in pointed end off-rate in the same experiment (see below).

Before continuing with studies involving addition of DBP, the effect of DBP on the binding between chick ADF and G-actin was determined. Non-denaturing gels were used to quantify the effect of adding DBP to ADF−actin complex. DBP binds tightly to actin monomer with a dissociation constant in the low nanomolar range (*69*), about 100−1000-fold tighter binding than ADF. The DBP binding site on actin reported from crystal structure (*70*, *71*) overlaps with the ADF binding site on actin predicted from molecular dynamics simulation (*72*). Thus, as expected, DBP quantitatively displaced ADF from ADF−actin complex (Supporting Information Figure 2). Therefore, in filament depolymerization assays, the addition of DBP will displace AC from G-actin and allow it to bind again to filaments. Thus, as the actin depolymerizes, the AC/F-actin ratio will continually increase. Since ACs quench the enhanced fluorescence of assembled pyrene−actin (*10*), part of the loss of fluorescence in these depolymerization assays could arise from quenching and not depolymerization. However, as shown below, the initial depolymerization rates measured after DBP addition should be an accurate measure of depolymerization.

The severing/off-rate enhancement assay developed by Moriyama and Yahara (*64*) is based upon the change in fluorescence of a small amount of pyrene actin used as a label for assembly. Because the amount of pyrene actin is only 5% of the total actin and initial ratios of AC to total actin do not exceed 1:4, the maximum fluorescence change due to quenching should never exceed 25% of the total signal. However, the contribution of quenching to the initial

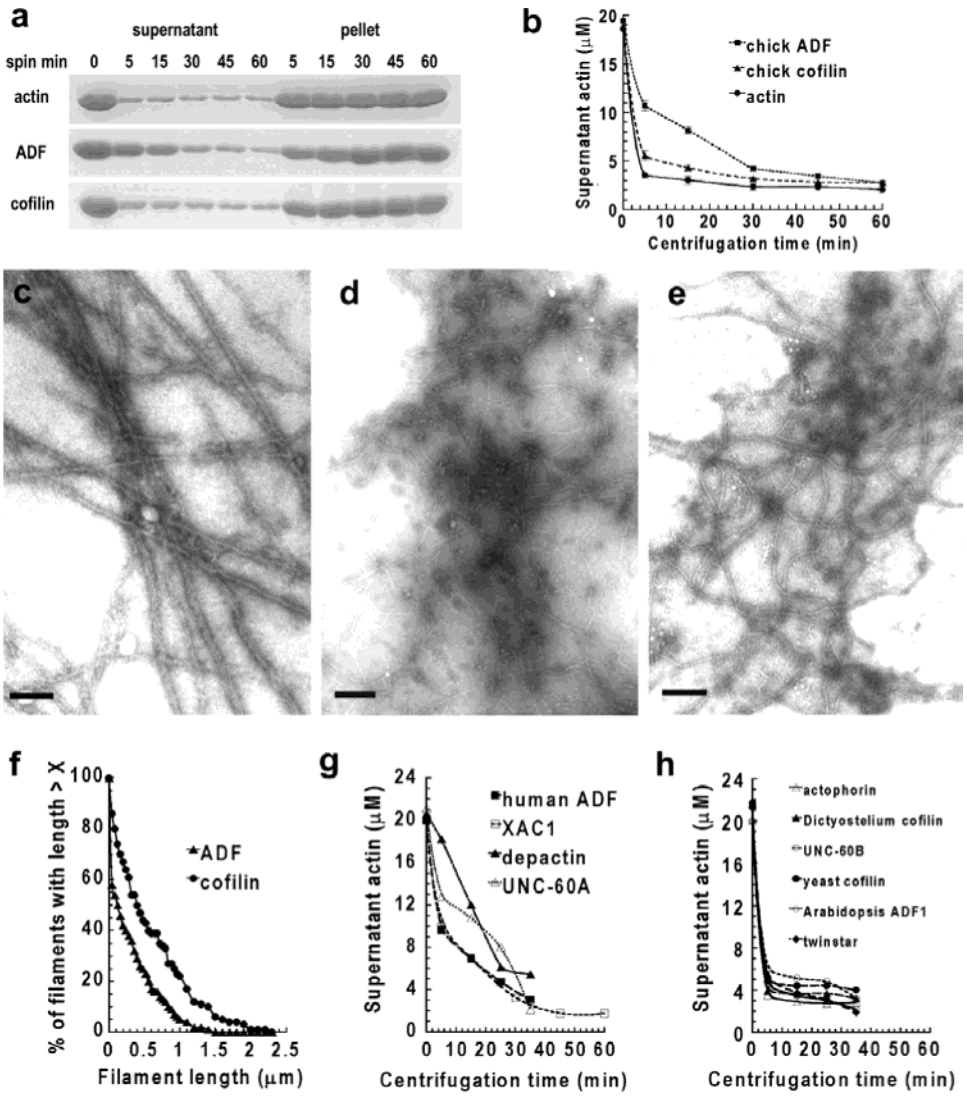

FIGURE 6: Timed sedimentation assay of steady-state mixtures of actin alone or in a 1:1 molar ratio with ADF or cofilin. Actin (20 μM) was polymerized to steady state in the presence or in the absence of ADF or cofilin at 4 °C in an ATP-regenerating buffer, pH 8.1, and centrifuged at 436000*g* for the times shown. The proteins in supernatants and solubilized pellets were separated by SDS−PAGE (a). The concentration of actin in the supernatant was plotted against the time of centrifugation (b). (c−f) The filament length distribution in the starting mixture was measured on negatively stained filaments before sedimentation using electron microscopy. Long filaments predominated in samples of actin alone (c) and actin plus cofilin (e), whereas short filaments predominated in samples of actin plus ADF (d). (f) The lengths of >100 filaments (105−191) treated with chick ADF (lower curve) or chick cofilin (upper curve) were measured from several different regions and from magnifications ranging from 15 000 to 75 000 and plotted as a distribution profile. Both curves fit exponential distributions for the filament length, but the slopes are different. (g) Timed sedimentation distribution of actin in the presence of ADF-like members of the AC family. (h) Timed sedimentation distribution of actin in the presence of cofilin-like members of the AC family.

fluorescence change is much less since before addition of DBP, samples are preincubated to allow quenching to reach a steady state (*64*). To be certain that our initial fluorescence measurements following addition of DBP were tracking filament depolymerization and not changes in quenching, we compared the depolymerization using both light scattering and fluorescence. When 5% of the total 3.3 μM actin is pyrene labeled and ADF is at 0.8 μM or less, light scattering and fluorescence assays gave identical initial depolymerization rates (Supporting Information Figure 3a−f). Because light scattering is much noisier than fluorescence, we quantified fluorescence in the depolymerization assays.

Because spontaneous actin nucleation is greater at lower pH, we nucleated actin assembly with gelsolin at pH 8 and then diluted the filaments to the appropriate final pH. A higher concentration of gelsolin−actin complex (154 vs 77 nM at pH 6.8) was required (determined experimentally) to cap the new filament ends generated at pH 7.8 because the severing activity of ADF and cofilin at pH 7.8 is greater than that at pH 6.8. With increasing concentrations of ADF or cofilin, the overall depolymerization rate of 3.3 μM actin was enhanced, reaching a maximum effect at about 0.6 μM ADF (Figure 8). At pH 6.8, cofilin (0.8 μM) increased the minus end off-rate from actin by 5-fold, whereas ADF (0.8 μM) increased the minus end off-rate 40-fold (Figure 8c,e). Both ADF and cofilin had only small effects on filament severing at pH 6.8 (major effects are on the slopes and not the intercept of the lines in Figure 8c), suggesting that the more rapid depolymerization observed for ADF over cofilin in the double-end-cap assay (Figure 7 and Table 3) arises from enhancing the off-rate and not from additional severing. At pH 7.8, cofilin (0.8 μM) did not significantly increase

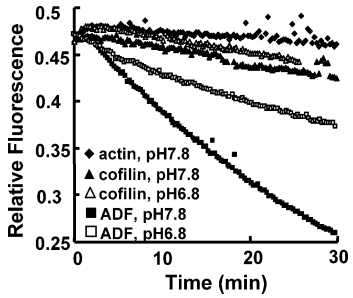

FIGURE 7: Effects of ADF and cofilin on the DBP-induced depolymerization of double-end-capped pyrene−actin filaments. Spectrin:actin:protein 4.1 complex (60 nM) was used to nucleate assembly of 3.3 μM actin containing 5% pyrene label. Steady state was reached within 10 min. Then 200 nM gelsolin:actin 1:1 complex was added along with nothing (actin control), 0.6 μM ADF (squares), or 0.6 μM cofilin (triangles). DBP was added after 10 min to induce depolymerization. Experiment was performed at pH 6.8 (open symbols) or 7.8 (closed symbols).

Table 3: Relative Initial Rate of Depolymerization of Double-End-Capped Filaments Compared to Actin Alone at Two pHs Following Treatment with Different ADF/Cofilins and Addition of DBP

ADF/cofilin protein	relative rate		ratio of rates
	pH 7.8	pH 6.8	pH 7.8/pH 6.8
yeast cofilin	55	10	5.5
Xenopus XAC1	29	9.6	3.0
Xenopus XAC2	25	6.8	3.7
chick ADF	22	11	2.0
depactin	15	6.0	2.5
Caenorhabditis UNC-60B	6.5	3.6	1.8
Dictyostelium cofilin	4.5	3.2	1.4
human ADF	3.9	4.4	0.9
Drosophila AC	3.8	4.3	0.9
Caenorhabditis UNC-60A	3.2	3.3	1.0
chick cofilin	2.8	3.8	0.7
Arabidopsis ADF1	2.6	2.1	1.2
Acanthomoeba actophorin	1.0	1.5	0.7

the minus end off-rate (no change in slope in Figure 8f), but it severed filaments to create an 8-fold increase in filament number. Under the same conditions, ADF increased the minus end off-rate 4-fold and increased filament number 20-fold (Figure 8f), a 2.5-fold difference in filament number that is similar to the 2-fold difference measured above (see Figure 6f) for average filament lengths between filaments treated with ADF or cofilin under identical conditions at high pH. Thus, the enhanced depolymerization rates observed for ADF over cofilin in the double-end-cap assay (Table 3) arises from both additional severing and enhanced off-rate. In summary, the filament depolymerizing activities of both chick ADF and chick cofilin are sensitive to pH, but ADF is more pH sensitive, and it enhances overall depolymerization (severing and off-rate enhancement) more effectively than chick cofilin.

Most AC Proteins Resemble either Chick ADF or Chick Cofilin in Their Interaction with Actin. Having established a series of assays that quantitatively distinguish between the in vitro behavior of ADF and cofilin, we applied several of these assays to other members of the AC family. Non-denaturing PAGE was used to determine the apparent dissociation constants of different AC proteins and G-actin. Under conditions of low ionic strength (calculated 34 μS), the nature of the actin-bound nucleotide and cation did not significantly affect the binding of XAC1 to G-actin, and the $K_{D\,app}$'s ranged from 0.4 to 0.8 μM (Table 1). Thus, XAC1 (*7*) behaved like chick ADF. *Drosophila* AC (tsr) (*6*), *Acanthomoba* actophorin (*73*, *74*), *Arabidopsis* ADF1 (*10*), and *Caenorhabditis* UNC-60B (*46*, *75*) had high-affinity binding ($K_{D\,app} \approx 0.5-3.8$ μM) similar to those of Mg^{2+}−ADP−actin, Ca^{2+}−ADP−actin, and Ca^{2+}−ADP−actin, but their $K_{D\,app}$'s for Mg^{2+}−ATP−actin were >16 μM (Table 1). Furthermore, free actin decreased or disappeared without a corresponding increase in the amount of complex, suggesting that these AC proteins nucleated assembly, and thus they behaved like chick cofilin. Equimolar mixtures of actin with each of the different AC proteins were used in a timed sedimentation assay at physiological ionic strength and pH 8.1 to estimate the distribution of filament lengths in the presence of an ATP-regenerating system. Less than 50% of the total actin was pelleted after a 5 min centrifugation, and heterogeneous filament distributions were observed when human ADF, *Xenopus* XAC1, starfish depactin (*76*), and *Caenorhabditis* UNC-60A (*46*, *75*) were used. These proteins behaved similarly to chick ADF (Figure 6g). *Acanthamoeba* actophorin, *Dictyostelium* cofilin (*77*), *Caenorhabditis* UNC-60B, yeast cofilin, *Arabidopsis* ADF1, and *Drosophila* AC behave like chick cofilin in this assay (Figure 6h). The pH-dependent depolymerizing activity of the different AC proteins was measured using an equal concentration (0.6 μM) of each protein in the double-end-cap filament depolymerization assay (Table 3). The activities of these proteins fell into two quantitatively different groups. Actin treated with chick ADF, XAC1, XAC2, yeast cofilin, and depactin had depolymerization rates relative to actin alone that were increased greater than 15-fold at pH 7.8 and greater than 6-fold at pH 6.8. The depolymerization rates for these ACs were 2−4-fold faster at pH 7.8 than at pH 6.8 (Table 3). Chick cofilin, actophorin, UNC-60B, UNC60A, *Drosophila* AC, *Arabidopsis* ADF1, *Dictyostelium* cofilin, and human ADF had depolymerization rates less than 7-fold greater than that of actin alone at pH 7.8 and less than 4-fold greater at pH 6.8, with less than a 2-fold difference in rates between pH 7.8 and 6.8.

There are three AC proteins that do not behave like the other members of the ADF or cofilin subgroup in all of the assays. Yeast cofilin showed the greatest pH-dependent depolymerizing behavior of any of the AC proteins (Table 3) but behaved like chick cofilin in the timed sedimentation assay (Figure 6 g). Human ADF and *Caenorhabditis* UNC-60A had weak filament depolymerization activities in the double-end-cap assay (Table 3) but behaved like chick ADF in generating a heterogeneous mixture of filament lengths in the timed sedimentation assay (Figure 6h).

DISCUSSION

Chick ADF, but Not Chick Cofilin, May Act as an ATP−G-Actin Sequestering Protein. Previous studies suggested that AC proteins do not act as major G-actin sequestering proteins in vivo because the monomeric actin pool in vivo is predominantly ATP−actin (*78*) and several AC proteins have 30−80-fold weaker affinities for Mg^{2+}−ATP−actin than for Mg^{2+}−ADP−actin under physiologically ionic conditions (*10*, *19*, *20*, *79*). Here, using non-denaturing PAGE and no protein modification, we find that the affinity of chick cofilin for Mg^{2+}−ATP−actin was >20-fold weaker than for Mg^{2+}−ADP−actin, qualitatively consistent with the previous results.

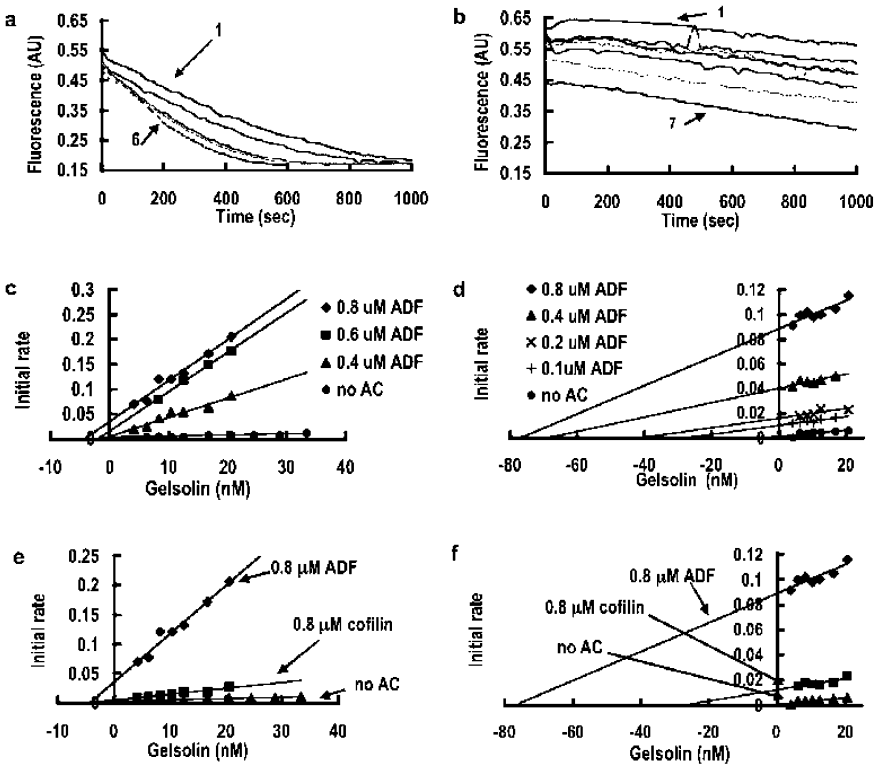

FIGURE 8: pH-dependent pointed-end depolymerization and severing of F-actin by ADF and cofilin. Gelsolin (4.125, 6.19, 8.25, 10.31, 12.36, 16.5, and 20.4 nM, panels a and b, top to bottom curves, respectively) nucleated F-actin (3.3 μM, 5% pyrene label) was preincubated with 77 nM gelsolin:actin 1:1 complex and (a) ADF (0.8 μM) or (b) cofilin (0.8 μM). The initial rate of fluorescence decrease following addition of 3.5 μM DBP is shown. The initial depolymerization rates of 3.3 μM F-actin treated with different concentrations of ADF at pH 6.8 (c) and 7.8 (d) are plotted against the starting gelsolin concentration (the actual concentration of free pointed ends was calculated to be 8.5% of the total gelsolin concentration). At both pH 6.8 (e) and pH 7.8 (f), ADF is more effective than cofilin at increasing the off-rate (slope of line) and at severing filaments (intercept on abcissa).

However, chick ADF has only a 2−4-fold difference in apparent affinity in binding Mg^{2+}−ADP−actin and Mg^{2+}−ATP−actin at ionic strengths from 20 to 90 μS. Given their relative affinities for ATP−actin and their intracellular concentrations in the 10−25 μM range (*80*; reviewed in ref *1*), our results suggest that chick ADF would act as an actin monomer sequestering protein whereas cofilin would not. Indeed, the monomer sequestering activity of ADF was demonstrated in extracts of embryonic chick brain, where the actin monomer binding proteins were examined on a DNase I affinity column (*81*). Even though both ADF and cofilin are present in significant amounts in these brain extracts, only ADF was found bound to monomer, and it is present in amounts sufficient to sequester close to 20% of the actin monomer pool (*81*). Thus, chick ADF and chick cofilin, though they share 70% sequence identity, function differently in brain cells.

It is interesting to note that the interaction between cofilin and ATP− vs ADP−G-actin is also affected by the divalent cation bound to the actin. When Mg^{2+} is bound, there is a 20-fold decrease in the apparent affinity of cofilin for ATP−actin which does not occur if Ca^{2+} is bound. The actin monomer has about a 4−5-fold higher affinity for Ca^{2+} over Mg^{2+} (*82*), but in resting cells, free intracellular Mg^{2+} (~0.5 mM) is more than 3000-fold higher than free intracellular Ca^{2+} (40−130 nM) (*83*, *84*). Thus, the predominant actin-bound divalent cation will be Mg^{2+} inside resting cells, as has been confirmed (*85*). However, in some microdomains of the cell, Ca^{2+} concentrations may transiently rise to >300 μM (*86*). Within these domains, especially in cortical areas underlying calcium channels, a significant portion of the actin could possibly exist, albeit transiently, in the Ca^{2+} form. Where Ca^{2+}−actin exists as a component of the actin pool, cofilin could transiently sequester ATP−actin in cortical regions.

A conformational alteration has been observed on going from the Ca^{2+} to the Mg^{2+} form of monomeric actin (*87*), perhaps due to exclusion of water molecules from the nucleotide binding pocket (*88*). The large difference in the apparent affinity of ADF and cofilin with Mg^{2+}−ATP actin, but not Ca^{2+}−ATP actin, suggests that this conformational change in actin affects only the cofilin binding. Thus, there is at least a subtle difference in the way these two AC proteins bind actin monomer.

Chick ADF Is More Effective in pH-Dependent Filament Depolymerization, and Chick Cofilin Is More Effective in Promoting Filament Assembly. Based on the amino acid sequence alignment, there is about a 70% sequence identity between ADF and cofilin-1/2 and 92% sequence identity between cofilin-1 and cofilin-2 (*47*). Mouse ADF is most efficient in promoting pH-dependent actin filament disassembly, followed by mouse cofilin-1. Mouse cofilin-2 was far less effective than the others (*47*). Studies comparing human ADF and human cofilin-1 detected only small differences in activities for actin filament binding and severing (*48*). Only one ADF and one cofilin have been identified in chick, and chick cofilin should be classified as cofilin-2 on the basis of its 98% sequence identity to mouse

and human cofilin-2 (*47*). Thus, our comparative study represents differences between ADF and cofilin-2.

Whether all AC proteins sever actin filaments has been controversial. In early studies of chick ADF and porcine cofilin, a filament severing activity was detected (*16*, *17*), suggesting that one mechanism for enhanced depolymerization was the generation of additional filament ends. The number of filaments eventually declined (*16*), suggesting annealing or subunit redistribution had occurred. However, Carlier et al. (*10*) reported that recombinant *Arabidopsis* ADF1 enhanced both the association rate (up to 12-fold) at the barbed ends of filaments and the dissociation rate (up to 22-fold) at filament pointed ends at pH 7.8 in the apparent absence of filament severing. Other workers reported less of an effect on subunit off-rates and more severing activity with human ADF, *Acanthamoeba* actophorin, *Dictyostelium* cofilin, and porcine cofilin (*42*, *64*, *89*). Some of these differences in AC activity could be due to a weaker severing activity of recombinant proteins compared to tissue-derived proteins (*89*), but as demonstrated here, it is most likely due to inherent differences in the proteins themselves.

Moriyama and Yahara (*64*) developed a novel assay that looked at both filament number (by trapping with a barbed-end capping complex) and rate of subunit loss from the uncapped pointed end. They found that porcine cofilin increased filament number by severing filaments with a maximum of about one severing event per 290 actin subunits at pH 7.1. Subunit off-rates were also enhanced to a maximum of about 6.4-fold. Mutant forms of cofilin were identified that differentially affected severing or the off-rate at the pointed end. Yeast cells expressing mutant cofilin with defects in severing are more impaired in their growth than those with defects in off-rate enhancement (*64*), suggesting that the ability of AC to sever is an essential process. Severing and off-rate enhancement are two separable processes that account for the enhanced filament turnover rate by AC.

Previous severing assays have relied on filaments settled onto glass coverslips (*42*, *89*, *90*) and have been subject to criticism that the severing is a result of restricting the ability of the actin to twist and flex (*91*). Here, we further developed an assay to measure the overall depolymerization rate (severing plus off-rate enhancement) by ADF or cofilin (Table 3). Since both ends of actin filaments are capped at the start of this assay, filament ends become available only if severing occurs. Results confirm the fact that both ADF and cofilin can sever F-actin in solution. Chick ADF is more effective in enhancing the depolymerization rate of filaments than chick cofilin, and the depolymerization rate is enhanced more at alkaline pH. In addition, *Arabidopsis thaliana* ADF1, previously reported not to sever F-actin (*10*), does have some severing activity in our assay, although it is among the weakest of the AC proteins. Using the assay of Moriyama and Yahara (*64*), we obtained results consistent with chick ADF being more effective than chick cofilin in both filament severing and minus end off-rate enhancement, as well as being more pH-dependent. For chick ADF, severing appears to account for most of the enhanced depolymerizing activity at alkaline pH, and off-rate enhancement from the pointed end appears to account for most of the enhanced depolymerizing activity at acidic pH (Figure 8). These results are somewhat different than those of Yeoh et al. (*48*), who used a different assay to show that severing of filaments by human ADF was not very pH-dependent. We also obtained no pH difference for human ADF in the double-end-capped filament depolymerization assay but did see a marked pH effect on chick ADF (Table 3). Whether these findings represent a functional difference between chick and human ADF or an unexplained difference in the assays is not yet clear. Nevertheless, what is quite clear from comparative results using the same assay is that chick ADF and human ADF are more effective than chick cofilin at increasing overall filament depolymerization.

The different severing and monomer sequestering properties of ADF and cofilin can also be used to explain why actin assembly occurred in the non-denaturing gel electrophoresis studies of cofilin−actin complexes. ADF will bind to ATP−actin monomer and prevent filament assembly up to 5 μM actin, because the critical concentration for ADF−actin assembly is above this concentration. However, the weak binding of chick cofilin to Mg^{2+}−ATP−actin could allow spontaneous nucleation to occur at 5 μM actin. These nuclei could serve to generate short pieces of ADP−F-actin to which cofilin can bind and sever, thus generating many more nuclei for filament growth. Thus, actin monomer disappears from these gels, not by forming a 1:1cofilin−actin complex, but rather by forming filaments that fail to enter the gel. By decreasing the actin monomer concentration to 2 μM, spontaneous nucleation was suppressed at the low ionic strength of the gel buffer, and the binding of cofilin to ATP−actin could then be measured.

Possible Structural Basis for the pH-Dependent Activity of Some ADF and Cofilin Proteins. For some proteins that show pH sensitivity over the physiological pH range of about 6.5−7.5, alterations in the ionization of histidine side chains are often responsible (*92*, *93*). The only histidine 133 of human cofilin has been suggested to convey the pH sensitivity by involving a salt bridge between His133 and Asp98 (*94*). An additional His70 is present in human and chick ADF and might convey the higher degree of pH sensitivity observed by Yeoh et al. (*48*). His70 is in the vicinity of a C-terminal-stabilizing interaction between residues Phe160 and Phe68 proposed by Bowman et al. (*95*). The C-terminus of ADF/cofilin has been implicated in F-actin binding (*96*, *97*). We inspected the structure of human ADF (1ak7), yeast cofilin (1qpv), and Acanthomoeba actophorin (1ahq) using the RasMol program (http://www.umass.edu/microbio/rasmol) and compared the location of histidine residues in different AC proteins on the basis of their structural homologies. All of the AC proteins with strong pH-dependent severing/depolymerizing activity have a histidine residue in the vicinity of the C-terminal-stabilizing interaction between residues 161 and 68. These include His70 of human ADF and chick ADF on the surface of helix 2, His22 of XAC1 and XAC2 on the surface of helix 1′, His85 of depactin in a loop between the β-strands 4 and 5, and a C-terminal His in yeast cofilin. In our assays, these proteins showed the greatest pH dependency.

Biochemical Results Help Explain Different Cellular Properties of ADF and Cofilin. Here we show that proteins in the ADF group have greater overall depolymerizing activities than proteins in the cofilin group, and they bind to Mg^{2+}−ATP−G-actin with higher affinity. Proteins in the cofilin group enhance nucleation. Members of both sub-

groups have been shown to enhance the filament turnover in vivo that is important for cell growth, motility, cytokinesis, endocytosis, and exocytosis. However, in multicellular organisms, the extent of actin filament turnover and mode of regulation needed are certain to vary depending on the species, cell type, and developmental stage, and thus either require different members of the AC family or other proteins that can alter AC behavior. One such modulator of AC activity is actin interacting protein 1 (Aip1) (*98*−*100*). In *C. elegans*, the Aip1 protein (unc78) enhances the activity of the muscle-specific unc60B (equivalent to cof-2) but has only minimal effects on the activity of the more ubiquitous unc60A (*101*), suggesting that even in multicellular organisms expressing different forms of AC proteins, alternative ways of modulating their function have continued to evolve.

The quantitative differences in vitro between ADF and cofilin in filament depolymerization can make a difference in filament organization in cells in which these proteins are overexpressed. Overexpressing the active and non-phosphorylatable XAC(A3)-GFP, a member of the ADF group with a significant affinity for Mg^{2+}−ATP−actin, causes cells to gradually round up and lose their ability to adhere to the substratum as expression increases, suggesting that the assembled actin pool is decreased (*1*). In contrast, overexpression of *Dictyostelium* cofilin, a member of the cofilin group, which has little affinity for Mg^{2+}−ATP−G-actin, caused an increase in F-actin and little change in G-actin (*102*). The overexpression of cofilin also stimulated cell motility and membrane ruffling, suggesting that enhanced filament dynamics can accompany an increase in F-actin. In cells that coexpress ADF and cofilin, these proteins might work cooperatively to enhance filament turnover. Indeed, results from a recent study by Dai et al. (*49*) suggest that temporal regulation of ADF and cofilin occur during *Salmonella* invasion of HeLa cells. Although both proteins undergo similar changes in their activation/inactivation by phospho-regulation during the invasion process, overexpressing the active non-phosphorylatable mutant form of either ADF or cofilin alone had no inhibitory effect on *Salmonella* uptake, whereas expressing similar total amounts of both active forms was inhibitory. These results suggest that the proteins have distinct (non-overlapping) functions in a process involving dynamic reorganization of cortical actin.

Wounding a monolayer of cells transiently increases intracellular pH and induces a translocation of ADF, cofilin, and actin to the edge of newly expanded lamellipodia (*43*). Blockage of the transient alkaline shift blocks lamellipodial expansion at the leading edge. Lamellipodial expansion is an actin assembly driven process that requires the exposure of barbed ends. The transient alkaline shift could activate the severing activity of ADF and induce more free barbed ends for filament assembly. The pH-induced changes in lamellipodial expansion could be due to pH-sensitive proteins other than ADF. However, two independent methods of inactivating ADF/cofilin that inhibit filament barbed-end generation at the leading edge (*103*, *104*) strongly suggest that AC proteins play a major role in barbed-end generation in some cell types.

In addition, shifting the intracellular pH of cultured cells alters the distribution of AC proteins relative to actin (*43*). At intracellular pH ~6.6, most of the ADF and cofilin co-localize with F-actin. However, at pH 7.4, cofilin and F-actin maintained their co-localization, but the co-localization of ADF and F-actin decreased by 30%. Thus, the pH-dependent differences between these proteins observed in vitro explains their behavior in vivo.

ACKNOWLEDGMENT

We thank Dr. Kris Gunsalus for working with us to purify *Drosophila* ADF/cofilin from her expression vector, Drs. Sharon Ashworth and Chris Staiger for providing the expression plasmid for *Arabidopsis* ADF1 and some of the recombinant ADF1 protein, Dr. Hiroshi Abe for providing the expression plasmids for *Xenopus* XAC1 and XAC2, Dr. Alan Weeds for providing expression plasmid for gelsolin, and Drs. Laurent Blanchoin, Shoichio Ono, John Condeelis, David Drubin, and Issei Mabuchi for providing recombinant *Acanthamoeba* actophorin, recombinant *Caenorhabditis* UNC-60A and UNC-60B, recombinant *Dictyostelium* cofilin, recombinant yeast cofilin, and endogenous starfish depactin, respectively. We gratefully acknowledge the gift of spectrin:actin:protein 4.1 from James Casella and Susan Craig. We also thank Sharon Kelly and Aimin Tang for technical assistance.

SUPPORTING INFORMATION AVAILABLE

Non-denaturing gel electrophoresis and Job plots of ADF/cofilin−actin complexes, showing that maximum complex formation occurs at a 1:1 molar ratio of actin to each of the ADF/cofilins; competition between DBP and ADF for binding to actin monomer; comparison of depolymerization measured by light scattering and pyrene−actin fluorescence. This material is available free of charge via the Internet at http://pubs.acs.org.

REFERENCES

1. Bamburg, J. R. (1999) Proteins of the ADF/Cofilin family: essential regulators of actin dynamics, *Annu. Rev. Cell Dev. Biol. 15*, 185−230.
2. Bamburg, J. R., and Bray, D. (1987) Distribution and cellular localization of actin depolymerizing factor, *J. Cell Biol. 105*, 2817−2825.
3. Yonezawa, N., Nishida, E., Koyasu, S., Maekawa, S., Ohta, Y., Yahara, I., and Sakai, H. (1987) Distribution among tissues and intracellular localization of cofilin, a 21kDa actin-binding protein, *Cell Struct. Funct. 12*, 443−452.
4. Moon, A. L., Janmey, P. A., Louie, K. A., and Drubin, D. G. (1993) Cofilin is an essential component of the yeast cortical cytoskeleton, *J. Cell Biol. 120*, 421−435.
5. Nagaoka, R., Kusano, K., Abe, H., and Obinata, T. (1995) Effects of cofilin on actin filamentous structures in cultured muscle cells. Intracellular regulation of cofilin action, *J. Cell Sci. 108*, 581−593.
6. Gunsalus, K. C., Bonaccorsi, S., Williams, E., Verni, F., Gatti, M., and Goldberg, M. L. (1995) Mutations in twinstar, a *Drosophila* gene encoding a cofilin/ADF homologue, result in defects in centrosome migration and cytokinesis, *J. Cell Biol. 131*, 1243−1259.
7. Abe, H., Obinata, T., Minamide, L. S., and Bamburg, J. R. (1996) *Xenopus laevis* actin-depolymerizing factor/cofilin: a phosphorylation-regulated protein essential for development, *J. Cell Biol. 132*, 871−885.
8. Lappalainen, P., and Drubin, D. G. (1997) Cofilin promotes rapid actin filament turnover in vivo, *Nature 388*, 78−82.
9. Rosenblatt, J., Agnew, B. J., Abe, H., Bamburg, J. R., and Mitchison, T. J. (1997) *Xenopus* actin depolymerizing factor/cofilin (XAC) is responsible for the turnover of actin filaments in *Listeria monocytogenes* tails, *J. Cell Biol. 136*, 1323−1332.

10. Carlier, M. F., Laurent, V., Santolini, J., Melki, R., Didry, D., Xia, G. X., Hong, Y., Chua, N. H., and Pantaloni, D. (1997) Actin depolymerizing factor (ADF/cofilin) enhances the rate of filament turnover: implication in actin-based motility, *J. Cell Biol. 136*, 1307−1322.
11. Loisel, T. P., Boujemaa, R., Pantaloni, D., and Carlier, M. F. (1999) Reconstitution of actin-based motility of Listeria and Shigella using pure proteins, *Nature 401*, 613−616.
12. Condeelis, J. S. (2001) How is actin polymerization nucleated *in vivo*? *Trends Cell Biol. 11*, 288−293.
13. Dawe, H. R., Minamide, L. S., Bamburg, J. R., and Cramer, L. P. (2003) ADF/cofilin controls cell polarity during fibroblast migration, *Curr. Biol. 13*, 252−257.
14. McGough, A., Pope, B., Chiu, W., and Weeds, A. (1997) Cofilin changes the twist of F-actin: implications for actin filament dynamics and cellular function, *J. Cell Biol. 138*, 771−781.
15. Galkin, V. E., Orlova, A., Lukoyanova, N., Wriggers, W., and Egelman, E. H. (2001) Actin depolymerizing factor stabilizes an existing state of F-actin and can change the tilt of F-actin subunits, *J. Cell Biol. 153*, 75−86.
16. Hayden, S. M., Miller, P. S., Brauweiler, A., and Bamburg, J. R. (1993) Analysis of the interactions of actin depolymerizing factor with G- and F-actin, *Biochemistry 32*, 9994−10004.
17. Nishida, E., Maekawa, S., and Sakai, H. (1984) Cofilin, a protein in porcine brain that binds to actin filaments and inhibits their interactions with myosin and tropomyosin, *Biochemistry 23*, 5307−5313.
18. Hawkins, M., Pope, B., Maciver, S. K., and Weeds, A. G. (1993) Human actin depolymerizing factor mediates a pH-sensitive destruction of actin filaments, *Biochemistry 32*, 9985−9993.
19. Blanchoin, L., and Pollard, T. D. (1998) Interaction of actin monomers with *Acanthamoeba* actophorin (ADF/cofilin) and profilin, *J. Biol. Chem. 273*, 25106−25111.
20. Ressad, F., Didry, D., Xia, G. X., Hong, Y., Chua, N. H., Pantaloni, D., and Carlier, M. F. (1998) Kinetic analysis of the interaction of actin-depolymerizing factor (ADF)/cofilin with G- and F-actins. Comparison of plant and human ADFs and effect of phosphorylation, *J. Biol. Chem. 273*, 20894−20902.
21. Yonezawa, N., Nishida, E., Iida, K., Yahara, I., and Sakai, H. (1990) Inhibition of the interactions of cofilin, destrin, and deoxyribonuclease I with actin by phosphoinositides, *J. Biol. Chem. 265*, 8382−8386.
22. Bernstein, B. W., and Bamburg, J. R. (1982) Tropomyosin binding to F-actin protects the F-actin from disassembly by brain actin-depolymerizing factor (ADF), *Cell Motil. 2*, 1−8.
23. Nishida, E., Muneyuki, E., Maekawa, S., Ohta, Y., and Sakai, H. (1985) An actin-depolymerizing protein (destrin) from porcine kidney. Its action on F-actin containing or lacking tropomyosin, *Biochemistry 24*, 6624−6630.
24. Bryce, N. S., Schevzov, G., Ferguson, V., Percival, J. M., Lin, J. J., Matsumura, F., Bamburg, J. R., Jeffrey, P. L., Hardeman, E. C., Gunning, P., and Weinberger, R. P. (2003) Specification of actin filament function and molecular composition by tropomyosin isoforms, *Mol. Biol. Cell 14*, 1002−1016.
25. Agnew, B. J., Minamide, L. S., and Bamburg, J. R. (1995) Reactivation of phosphorylated actin depolymerizing factor and identification of the regulatory site, *J. Biol. Chem. 270*, 17582−17587.
26. Smertenko, A. P., Jiang, C. J., Simmons, N. J., Weeds, A. G., Davies, D. R., and Hussey, P. J. (1998) Ser6 in the maize actin-depolymerizing factor, ZmADF3, is phosphorylated by a calcium-stimulated protein kinase and is essential for the control of functional activity, *Plant J. 14*, 187−193.
27. Blanchoin, L., Robinson, R. C., Choe, S., and Pollard, T. D. (2000) Phosphorylation of *Acanthamoeba* actophorin (ADF/cofilin) blocks interaction with actin without a change in atomic structure, *J. Mol. Biol. 295*, 203−211.
28. Arber, S., Barbayannis, F. A., Hanser, H., Schneider, C., Stanyon, C. A., Bernard, O., and Caroni, P. (1998) Regulation of actin dynamics through phosphorylation of cofilin by LIM-kinase, *Nature 393*, 805−809.
29. Yang, N., Higuchi, O., Ohashi, K., Nagata, K., Wada, A., Kangawa, K., Nishida, E., and Mizuno, K. (1998) Cofilin phosphorylation by LIM-kinase 1 and its role in Rac-mediated actin reorganization, *Nature 393*, 809−812.
30. Sumi, T., Matsumoto, K., Takai, Y., and Nakamura, T. (1999) Cofilin phosphoylation and actin cytoskeletal dynamics regulated by Rho- and Cdc42-actiated LIM-kinase 2, *J. Cell Biol. 147*, 1519−1532.
31. Maekawa, M., Ishizaki, T., Boku, S., Watanabe, N., Fujita, A., Iwamatsu, A., Obinata, T., Ohashi, K., Mizuno, K., and Narumiya, S. (1999) Signaling from Rho to the actin cytoskeleton through protein kinases ROCK and LIM-kinase, *Science 285*, 895−898.
32. Amano, T., Tanabe, K., Eto, T., Narumiya, S., and Mizuno, K. (2001) LIM-kinase 2 induces formation of stress fibres, focal adhesions and membrane blebs, dependent on its activation by Rho-associated kinase-catalysed phosphorylation at threonine-505, *Biochem. J. 354*, 149−159.
33. Toshima, J., Toshima, J. Y., Amano, T., Yang, N., Narumiya, S., and Mizuno, K. (2001) Cofilin phosphorylation by protein kinase testicular protein kinase 1 and its role in integrin-mediated actin reorganization and focal adhesion formation, *Mol. Biol. Cell 12*, 1131−1145.
34. Toshima, J., Toshima, J. Y., Takeuchi, K., Mori, R., and Mizuno, K. (2001) Cofilin phosphorylation and actin reorganization activities of testicular protein kinase 2 and its predominant expression in testicular Sertoli cells, *J. Biol. Chem. 276*, 31449−31458.
35. Toshima, J., Toshima, J. Y., Amano, T., Yang, N., Narumiya, S., and Mizuno, K. (2001) Cofilin phosphorylation by protein kinase testicular protein kinase 1 and its role in integrin-mediated actin reorganization and focal adhesion formation, *Mol. Biol. Cell 12*, 1131−1145.
36. Gohla, A., and Bokoch, G. M. (2002) 14-3-3 regulates actin dynamics by stabilizing phosphorylated cofilin, *Curr. Biol. 12*, 1704−1710.
37. Birkenfeld, J., Betz, H., and Roth, D. (2003) Identification of cofilin and LIM-domain-containing protein kinase 1 as novel interaction partners of 14-3-3 zeta, *Biochem. J. 369*, 45−54.
38. Toshima, J. Y., Toshima, J., Watanabe, T., and Mizuno, K. (2001) Binding of 14−3−3beta regulates the kinase activity and subcellular localization of testicular protein kinase 1, *J. Biol. Chem. 276*, 43471−43481.
39. Niwa, R., Nagata-Ohashi, K., Takeichi, M., Mizuno, K., and Uemura, T. (2002) Control of actin reorganization by Slingshot, a family of phosphatases that dephosphorylate ADF/cofilin, *Cell 108*, 233−246.
40. Ohta, Y., Kousaka, K., Nagata-Ohashi, K., Ohashi, K., Muramoto, A., Shima, Y., Niwa, R., Uemura, T., and Mizuno, K. (2003) Differential activities, subcellular distribution and tissue expression patterns of three members of Slingshot family phosphatases that dephosphorylate cofilin, *Genes Cells 8*, 811−824.
41. Bamburg, J. R., and Wiggan, O. P. (2002) ADF/cofilin and actin dynamics in disease, *Trends Cell Biol. 12*, 598−605.
42. Maciver, S. K., Pope, B. J., Whytock, S., and Weeds, A. G. (1998) The effect of two actin depolymerizing factors (ADF/cofilins) on actin filament turnover: pH sensitivity of F-actin binding by human ADF, but not of *Acanthamoeba* actophorin, *Eur. J. Biochem. 256*, 388−397.
43. Bernstein, B. W., Painter, W. B., Chen, H., Minamide, L. S., Abe, H., and Bamburg, J. R. (2000) Intracellular pH modulation of ADF/cofilin proteins, *Cell Motil. Cytoskeleton 47*, 319−336.
44. Lappalainen, P., Kessels, M. M., Cope, M. J., and Drubin, D. G. (1998) The ADF homology (ADF−H) domain: a highly exploited actin-binding module, *Mol. Biol. Cell 9*, 1951−1959.
45. Iida, K., Moriyama, K., Matsumoto, S., Kawasaki, H., Nishida, E., and Yahara, I. (1993) Isolation of a yeast essential gene, COF1, that encodes a homologue of mammalian cofilin, a low-M(r) actin-binding and depolymerizing protein, *Gene 124*, 115−120.
46. Ono, S., and Benian, G. M. (1998) Two *Caenorhabditis elegans* actin depolymerizing factor/cofilin proteins, encoded by the unc-60 gene, differentially regulate actin filament dynamics, *J. Biol. Chem. 273*, 3778−3783.
47. Vartiainen, M. K., Mustonen, T., Mattila, P. K., Ojala, P. J., Thesleff, I., Partanen, J., and Lappalainen, P. (2002) The three mouse actin-depolymerizing factor/cofilins evolved to fulfill cell-type-specific requirements for actin dynamics, *Mol. Biol. Cell 13*, 183−194.
48. Yeoh, S., Pope, B., Mannherz, H. G., and Weeds, A. (2002) Determining the differences in actin binding by human ADF and cofilin, *J. Mol. Biol. 315*, 911−925.
49. Dai, S., Sarmiere, P. D., Wiggan, O., Bamburg, J. R., and Zhou, D. (2004) Efficient *Salmonella* entry requires activity cycles of host ADF and cofilin, *Cell Microbiol. 6*, 459−471.
50. Pardee, J. D., and Spudich, J. A. (1982) Purification of muscle actin, *Methods Enzymol. 85 Pt. B*, 164−181.

51. Kinosian, H. J., Selden, L. A., Estes, J. E., and Gershman, L. C. (1993) Nucleotide binding to actin. Cation dependence of nucleotide dissociation and exchange rates, *J. Biol. Chem. 268*, 8683−8691.
52. Gershman, L. C., Selden, L. A., Kinosian, H. J., and Estes, J. E. (1989) Preparation and polymerization properties of monomeric ADP-actin, *Biochim. Biophys. Acta 995*, 109−115.
53. Giuliano, K. A., Khatib, F. A., Hayden, S. M., Daoud, E. W., Adams, M. E., Amorese, D. A., Bernstein, B. W., and Bamburg, J. R. (1988) Properties of purified actin depolymerizing factor from chick brain, *Biochemistry 27*, 8931−8938.
54. Adams, M. E., Minamide, L. S., Duester, G., and Bamburg, J. R. (1990) Nucleotide sequence and expression of a cDNA encoding chick brain actin depolymerizing factor, *Biochemistry 29*, 7414−7420.
55. Abe, H., Ohshima, S., and Obinata, T. (1989) A cofilin-like protein is involved in the regulation of actin assembly in developing skeletal muscle, *J. Biochem. 106*, 696−702.
56. Nagaoka, R., Abe, H., and Obinata, T. (1996) Site-directed mutagenesis of the phosphorylation site of cofilin: its role in cofilin-actin interaction and cytoplasmic localization, *Cell Motil. Cytoskeleton 35*, 200−209.
57. Houk, T. W. J., and Ue, K. (1974) The measurement of actin concentration in solution: a comparison of methods, *Anal. Biochem. 62*, 66−74.
58. Gill, S. C., and von Hippel, P. H. (1989) Calculation of protein extinction coefficients from amino acid sequence data, *Anal. Biochem. 182*, 319−326.
59. Pope, B. J., Gooch, J. T., and Weeds, A. G. (1997) Probing the effects of calcium on gelsolin, *Biochemistry 36*, 15848−15855.
60. Gremm, D., and Wegner, A. (1999) Co-operative binding of Ca^{2+} ions to the regulatory binding sites of gelsolin, *Eur. J. Biochem. 262*, 330−334.
61. Huang, C. Y. (1982) Determination of binding stoichiometry by the continuous variation method: the Job plot, *Methods Enzymol. 87*, 509−525.
62. Laemmli, U. K. (1970) Cleavage of structural proteins during the assembly of the head of bacteriophage T4, *Nature 227*, 680−685.
63. McLeod, J. F., Kowalski, M. A., and Haddad, J. G., Jr. (1989) Interactions among serum vitamin D binding protein, monomeric actin, profilin, and profilactin, *J. Biol. Chem. 264*, 1260−1267.
64. Moriyama, K., and Yahara, I. (1999) Two activities of cofilin, severing and accelerating directional depolymerization of actin filaments, are differentially affected by mutations around the actin-binding helix, *EMBO J. 18*, 6752−6761.
65. Coluccio, L. M., and Tilney, L. G. (1984) Phalloidin enhances actin assembly by preventing monomer dissociation, *J. Cell Biol. 99*, 529−535.
66. Ralston, G. (1993) in *Introduction to analytical ultracentrifugation*, Beckman Instruments, Inc., Fullerton, CA.
67. Cantor, C. R., and Schimmel, P. R. (1980) in *Biophysical chemistry*, W. H. Freeman and Co., San Francisco.
68. Ressad, F., Didry, D., Egile, C., Pantaloni, D., and Carlier, M. F. (1999) Control of actin filament length and turnover by actin depolymerizing factor (ADF/Cofilin) in the presence of capping proteins and ARP2/3 complex, *J. Biol. Chem. 274*, 20970−20976.
69. Pollard, T. D., and Cooper, J. A. (1986) Actin and actin-binding proteins. A critical evaluation of mechanisms and functions, *Annu. Rev. Biochem. 55*, 987−1035.
70. Head, J. F., Swamy, N., and Ray, R. (2002) Crystal structure of the complex between actin and human vitamin D-binding protein at 2.5 A resolution, *Biochemistry 41*, 9015−9020.
71. Otterbein, L. R., Cosio, C., Graceffa, P., and Dominguez, R. (2002) Crystal structures of the vitamin D-binding protein and its complex with actin: structural basis of the actin-scavenger system, *Proc. Natl. Acad. Sci. U.S.A. 99*, 8003−8008.
72. Wriggers, W., Tang, J. X., Azuma, T., Marks, P. W., and Janmey, P. A. (1998) Cofilin and gelsolin segment-1: molecular dynamics simulation and biochemical analysis predict a similar actin binding mode, *J. Mol. Biol. 282*, 921−932.
73. Cooper, J. A., Blum, J. D., Williams, R. C. J., and Pollard, T. D. (1986) Purification and characterization of actophorin, a new 15,000-dalton actin-binding protein from *Acanthamoeba castellanii*, *J. Biol. Chem. 261*, 477−485.
74. Quirk, S., Maciver, S. K., Ampe, C., Doberstein, S. K., Kaiser, D. A., VanDamme, J., Vandekerckhove, J. S., and Pollard, T. D. (1993) Primary structure of and studies on *Acanthamoeba* actophorin, *Biochemistry 32*, 8525−8533.
75. McKim, K. S., Matheson, C., Marra, M. A., Wakarchuk, M. F., and Baillie, D. L. (1994) The *Caenorhabditis elegans* unc-60 gene encodes proteins homologous to a family of actin-binding proteins, *Mol. Gen. Genet. 242*, 346−357.
76. Mabuchi, I. (1983) An actin-depolymerizing protein (depactin) from starfish oocytes: properties and interaction with actin, *J. Cell Biol. 97*, 1612−1621.
77. Aizawa, H., Sutoh, K., Tsubuki, S., Kawashima, S., Ishii, A., and Yahara, I. (1995) Identification, characterization, and intracellular distribution of cofilin in *Dictyostelium discoideum*, *J. Biol. Chem. 270*, 10923−10932.
78. Rosenblatt, J., Peluso, P., and Mitchison, T. J. (1995) The bulk of unpolymerized actin in *Xenopus* egg extracts is ATP-bound, *Mol. Biol. Cell 6*, 227−236.
79. Maciver, S. K., and Weeds, A. G. (1994) Actophorin preferentially binds monomeric ADP-actin over ATP-bound actin: consequences for cell locomotion, *FEBS Lett. 347*, 251−256.
80. Koffer, A., Edgar, A. J., and Bamburg, J. R. (1988) Identification of two species of actin depolymerizing factor in cultures of BHK cells, *J. Muscle Res. Cell Motil. 9*, 320−328.
81. Devineni, N., Minamide, L. S., Niu, M., Safer, D., Verma, R., Bamburg, J. R., and Nachmias, V. T. (1999) A quantitative analysis of G-actin binding proteins and the G-actin pool in developing chick brain, *Brain Res. 823*, 129−140.
82. Estes, J. E., Selden, L. A., Kinosian, H. J., and Gershman, L. C. (1992) Tightly-bound divalent cation of actin, *J. Muscle Res. Cell Motil. 13*, 272−284.
83. Gasbarrini, A., Borle, A. B., Farghali, H., Bender, C., Francavilla, A., and Van Thiel, D. (1992) Effect of anoxia on intracellular ATP, Na^{+}i, Ca^{2+}i, Mg^{2+}i, and cytotoxicity in rat hepatocytes, *J. Biol. Chem. 267*, 6654−6663.
84. Zaffran, Y., Lepidi, H., Bongrand, P., Mege, J. L., and Capo, C. (1993) F-actin content and spatial distribution in resting and chemoattractant-stimulated human polymorphonuclear leucocytes. Which role for intracellular free calcium? *J. Cell Sci. 105*, 675−684.
85. Kitazawa, T., Shuman, H., and Somlyo, A. P. (1982) Calcium and magnesium binding to thin and thick filaments in skinned muscle fibres: electron probe analysis, *J. Muscle Res. Cell Motil. 3*, 437−454.
86. Llinas, R., Sugimori, M., and Silver, R. B. (1992) Microdomains of high calcium concentration in a presynaptic terminal, *Science 256*, 677−679.
87. Nyitrai, M., Hild, G., Belagyi, J., and Somogyi, B. (1997) Spectroscopic study of conformational changes in subdomain 1 of G-actin: influence of divalent cations, *Biophys. J. 73*, 2023−2032.
88. Fuller, N., and Rand, R. P. (1999) Water in actin polymerization, *Biophys. J. 76*, 3261−3266.
89. Ichetovkin, I., Han, J., Pang, K. M., Knecht, D. A., and Condeelis, J. S. (2000) Actin filaments are severed by both native and recombinant *Dictyostelium* cofilin but to different extents, *Cell Motil. Cytoskeleton 45*, 293−306.
90. Blanchoin, L., Pollard, T. D., and Mullins, R. D. (2000) Interactions of ADF/cofilin, Arp2/3 complex, capping protein and profilin in remodeling of branched actin filament networks, *Curr. Biol. 10*, 1273−1282.
91. Carlier, M. F., Ressad, F., and Pantaloni, D. (1999) Control of actin dynamics in cell motility. Role of ADF/cofilin, *J. Biol. Chem. 274*, 33827−33830 (review, 62 refs).
92. Mangs, H., Sui, G. C., and Wiman, B. (2000) PAI-1 stability: the role of histidine residues, *FEBS Lett. 475*, 192−196.
93. Linder, M., Nevanen, T., and Teeri, T. T. (1999) Design of a pH-dependent cellulose-binding domain, *FEBS Lett. 447*, 13−16.
94. Pope, B. J., Zierler-Gould, K. M., Kuhne, R., Weeds, A. G., and Ball, L. J. (2004) Solution structure of human cofilin: actin binding, pH sensitivity, and relationship to actin-depolymerizing factor, *J. Biol. Chem. 279*, 4840−4848.
95. Bowman, G. D., Nodelman, I. M., Hong, Y., Chua, N. H., Lindberg, U., and Schutt, C. E. (2000) A comparative structural analysis of the ADF/Cofilin family, *Proteins 41*, 374−384.
96. Lappalainen, P., Fedorov, E. V., Fedorov, A. A., Almo, S. C., and Drubin, D. G. (1997) Essential functions and actin-binding surfaces of yeast cofilin revealed by systematic mutagenesis, *EMBO J. 16*, 5520−5530.
97. Ono, S., McGough, A., Pope, B. J., Tolbert, V. T., Bui, A., Pohl, J., Benian, G. M., Gernert, K. M., and Weeds, A. G. (2001) The

C-terminal tail of UNC-60B (actin depolymerizing factor/cofilin) is critical for maintaining its stable association with F-actin and is implicated in the second actin-binding site, *J. Biol. Chem. 276*, 5952−5958.

98. Okada, K., Obinata, T., and Abe, H. (1999) XAIP1: a *Xenopus* homologue of yeast actin interacting protein 1 (AIP1), which induces disassembly of actin filaments cooperatively with ADF/cofilin family proteins, *J. Cell Sci. 112*, 1553−1565.
99. Okada, K., Blanchoin, L., Abe, H., Chen, H., Pollard, T. D., and Bamburg, J. R. (2002) Xenopus actin-interacting protein 1 (XAip1) enhances cofilin fragmentation of filaments by capping filament ends, *J. Biol. Chem. 277*, 43011−43016.
100. Balcer, H. I., Goodman, A. L., Rodal, A. A., Smith, E., Kugler, J., Heuser, J. E., and Goode, B. L. (2003) Coordinated regulation of actin filament turnover by a high-molecular-weight Srv2/CAP complex, cofilin, profilin, and Aip1, *Curr. Biol. 13*, 2159−2169.
101. Mohri, K., and Ono, S. (2003) Actin filament disassembling activity of *Caenorhabditis elegans* actin-interacting protein 1 (UNC-78) is dependent on filament binding by a specific ADF/cofilin isoform, *J. Cell Sci. 116*, 4107−4118.
102. Aizawa, H., Sutoh, K., and Yahara, I. (1996) Overexpression of cofilin stimulates bundling of actin filaments, membrane ruffling, and cell movement in *Dictyostelium*, *J. Cell Biol. 132*, 335−344.
103. Chan, A. Y., Bailly, M., Zebda, N., Segall, J. E., and Condeelis, J. S. (2000) Role of cofilin in epidermal growth factor-stimulated actin polymerization and lamellipod protrusion, *J. Cell Biol. 148*, 531−542.
104. Zebda, N., Bernard, O., Bailly, M., Welti, S., Lawrence, D. S., and Condeelis, J. S. (2000) Phosphorylation of ADF/Cofilin abolishes EGF-induced actin nucleation at the leading edge and subsequent lamellipod extension, *J. Cell Biol. 151*, 1119−1128.

BI049797N